İSTANBUL TECHNICAL UNIVERSITY ★ GRADUATE SCHOOL OF SCIENCE ENGINEERING AND TECHNOLOGY

APPLICATION OF HUMAN MESENCHYMAL STEM CELLS TO 3D SILK FIBROIN SCAFFOLDS FOR CARDIAC TISSUE ENGINEERING

M.Sc. THESIS

Gizem Merve ŞAHİN

Department of Molecular Biology-Genetics and Biotechnology

Molecular Biology-Genetics and Biotechnology Programme

JUNE 2017

İSTANBUL TECHNICAL UNIVERSITY ★ GRADUATE SCHOOL OF SCIENCE ENGINEERING AND TECHNOLOGY

APPLICATION OF HUMAN MESENCHYMAL STEM CELLS TO 3D SILK FIBROIN SCAFFOLDS FOR CARDIAC TISSUE ENGINEERING

M.Sc. THESIS

Gizem Merve ŞAHİN
(521141123)

Department of Molecular Biology-Genetics and Biotechnology

Molecular Biology-Genetics and Biotechnology Programme

Thesis Advisor: Assoc. Prof. Dr. Fatma Neşe KÖK
Thesis Co-Advisor: Dr. Yüksel ÇETİN

JUNE 2017

İSTANBUL TEKNİK ÜNİVERSİTESİ ★ FEN BİLİMLERİ ENSTİTÜSÜ

İNSAN MEZENKİMAL KÖK HÜCRELERİNİN 3B İPEK FİBROİN YAPI İSKELELERİNE UYGULANARAK KARDİYAK DOKU MÜHENDİSLİĞİNDE KULLANILMASI

YÜKSEK LİSANS TEZİ

Gizem Merve ŞAHİN
(521141123)

Moleküler Biyoloji-Genetik ve Biyoteknoloji Anabilim Dalı

Moleküler Biyoloji-Genetik ve Biyoteknoloji Programı

Tez Danışmanı: Doç. Dr. Fatma Neşe KÖK
Eş Danışman: Dr. Yüksel ÇETİN

HAZİRAN 2017

Gizem Merve ŞAHİN, a MSc student of ITU Graduate School of Science, Engineering and Technology student ID 521141123, successfully defended the thesis entitled "APPLICATION OF HUMAN MESENCHYMAL STEM CELLS TO 3D SILK FIBROIN SCAFFOLDS FOR CARDIAC TISSUE ENGINEERING", which she prepared after fulfilling the requirements specified in the associated legislations, before the jury whose signatures are below.

Thesis Advisor :	**Assoc. Prof. Dr. Fatma Neşe KÖK** İstanbul Technical University	.....
Co-advisor :	**Dr. Yüksel ÇETİN** TÜBİTAK MAM GMBE	.....
Jury Members :	**Prof. Dr. Fatma Seniha GÜNER** İstanbul Technical University	.....
	Prof. Dr. Nevin GÜL KARAGÜLER İstanbul Technical University	.....
	Assist. Prof. Dr. Fatih KOCABAŞ Yeditepe University	.....

Date of Submission : 05 May 2017
Date of Defense : 06 June 2017

To my family and friends,

FOREWORD

I would like to special thank my sincere gratitude to my supervisor Assoc. Prof. Dr. Fatma Nese KÖK; for her guidance, encouragement, patience, cheerfulness, and continuous support during my master programme. I also would like to express my sincere thanks to my second advisor Dr. Yüksel ÇETİN; for her guidance, endless support, motivation, and understanding of any problem that I went through. I could not get this step without their support and guidance.

I would also like to thank Assist Prof Sakip Önder for his time and support for scanning electron microscope images of scaffolds, and Dr. Ceyda Açılan Ayhan, Dr. Zelal Adıgüzel for their help and for allowing me to use equipments in their laboratories. In addition, I want to special thanks to dear İnas Özcan, and my lab-mates Burak Ağbaba, Ayşe Buse Özdabak, Arife Kuşbaz for their helps, supports and great friendships during my busy laboratory times.

A very special thank is to my previous manager, Kirstin Öztürk, who encouraged me to go back to an academic life, for always supporting me to achieve my goals in life. I would also like to acknowledge the financial support of Istanbul Technical University through Graduate Thesis Funding Project (grant no: 38894).

Running many tasks together can be a compelling circumstance sometimes. At this point, a huge bunch of loves goes to my dearest friends; Merve Yılmaz, Sümeyra Köstereli, Yeşim Yudum Mücaz. Additionally, I would like to express my endless thanks to Batuhan Demir who makes me feel strong for being always by my side in any case.

Above all, I would like to thank Coşkun Şahin, my father, Olcay Şahin, my mother, and my sisters for being in my life with their great supports in my actions, and ideas, and faith in me to make me a better person in life. I cannot imagine a life without them.

Mahatma Gandhi once said “Be the change that you wish to see in the world.” Thus, I dedicate this thesis to all women scientists who need to work harder, and to make a small change for a better world.

May 2017

Gizem Merve ŞAHİN
Bioengineer

TABLE OF CONTENTS

Page

ABBREVIATIONS

3D	**:** Three-dimensional
ADSC	**:** Adipose Derived Stem Cells
BSA	**:** Bovine Serum Albumin
$CaCl_2$	**:** Calcium Chloride
CO2	**:** Carbon Dioxide
CVD	**:** Cardio Vascular Diseases
DMEM-lg	**:** Dulbecco's Modified Eagle Medium-low glucose
DMSO	**:** Dimethyl Sulfoxide
DPBS	**:** Dulbecco's Phosphate-Buffered Saline
ECM	**:** Extra Cellular Matrix
et. al.	**:** et aliae
FBS	**:** Fetal Bovine Serum
hAD-MSC	**:** Human Adipose Derived Stem Cells
HCL	**:** Hydrochloric Acid
HLA-DR	**:** Human Leukocyte Antigen - antigen D Related
IF	**:** Immunofluorescence
IHC	**:** Immunohistochemistry
ISO 10993-12	**:** International Organization for Standardization; Biological Evaluation of Medical Device
ITS	**:** Insulin-Transferrin-Selenium
LiBr	**:** Lithium Bromide
MI	**:** Myocardial Infarction
MSC	**:** Mesenchymal Stem Cells
MTT	**:** 3-(4,5-Dimethylthiazol-2-Yl)-2,5-Diphenyltetrazolium Bromide
NaCl	**:** Sodium Chloride
Na_2CO_3	**:** Sodium Carbonate
NH_4Cl	**:** Ammonium Chloride
PBS	**:** Phosphate Buffered Saline
SEM	**:** Scanning Electron Microscopy
SF	**:** Silk Fibroin
UV	**:** Ultraviolet
WST-1	**:** Water Soluble Tetrazolium Salts-1

SYMBOLS

%	**:** Per cent
atm	**:** Atmosphere
g	**:** Gram
kDa	**:** Kilodalton
M	**:** Molar
mg	**:** Milligram
mL	**:** Mililitre
nm	**:** Nanometer
pH	**:** Power of Hydrogen
psi	**:** Pounds per Square Inch
rpm	**:** Revolutions per Minute
U/mL	**:** Units per Volume Solution Concentration
v/v %	**:** Volume/Volume per cent
w/v %	**:** Weight/Volume per cent
oC	**:** Degree Centigrade

LIST OF TABLES

Page

LIST OF FIGURES

Page

APPLICATION OF HUMAN MESENCHYMAL STEM CELLS TO 3D SILK FIBROIN SCAFFOLDS FOR CARDIAC TISSUE ENGINERING

SUMMARY

Cardiovascular diseases are the leading cause of death in the world. The risk of getting myocardial infarction (MI) is the highest rate (40.3 %) among deaths caused by cardiovascular diseases. MI causes loss of cardiomyocytes which lead to decrease in heart function. Since the regenerative capacity of cardiomyocytes is extremely low, damage becomes permanent in many patients. There are many treatments for this clinical problem such as using β-blockers, and ACE-inhibitors, AT1-receptor blockers, or organ transplantation at later stage, but number of patients with MI is increasing and current treatments are not effective enough to resolve this problem. At this point, development of the replacement tissue to replace or repair damaged area by tissue engineering techniques using patient's own cells on scaffolds has been explored as a lifesaving approach.

In this study, human adipose-derived mesenchymal stem cells (hAD-MSCs) and silk fibroin, a natural, biodegradable and biocompatible polymer, was chosen to regenerate damaged cardiac tissue after MI. 3D silk scaffolds were fabricated by freeze drying method, and effect of freezing conditions and insulation cover on pore structure was evaluated. After freeze drying process, silk scaffolds were exposed to methanol treatment to induce beta sheet structure from random coil structure which is also related with pore structure. Then, scaffolds were characterized for their water uptake capacity, morphology (scanning electron microscope (SEM)), biodegradation, and for their potential to sustain cell viability and proliferation tests. SEM results showed the change of pore structure by changing ratio of silk fibroin in the solution. According to results, the best two ratios in terms of pore structure, 2 % and 4 %, were chosen for next steps. Water uptake test showed high fluid uptake capacity of those silk fibroin scaffolds. To prevent excessive change in scaffold structure during application, scaffold with lower water uptake ratio was selected. Biodegradation test was performed for 14 days with 0.1 U/mL Protease IV to determine the biodegradation rate of scaffolds which is an essential parameter in tissue engineering. Silk fibroin scaffolds were degraded to about 50 % of their initial weight on day three, then biodegradation rate slowed down.

After the characterization of the scaffolds, mesenchymal stem cells were isolated from human adipose tissue which is a rare cell source for cardiac tissue engineering. hAD-MSCs are selected because of its ease of collection and high amount of cell obtained from a single operation. After the isolation procedure, characterization of mesenchymal stem cells was done with flow cytometry and immunohistochemistry analysis. Flow cytometry results showed that more than 90 % of the culture was characterized as MSC, indeed with high level of purity, and immunohistochemistry analysis proved the multi-differentiation capacity of hAD-MSCs into three different cell types; osteocytes, chondrocytes and adipocytes. Later, isolated and characterized hAD-MSCs were differentiated into cardiomyocytes with PSC Cardiomyocyte

Differentiation Kit to seed on silk scaffolds. Sarcomeric, ball-like structure was seen under inverted microscope, and differentiation of hAD-MSCs was proven with cardiac specific markers such as α-actinin, Troponin I, Connexin 43, and Myosin heavy chain by immunoflorecence analysis.

Ultimately, the biocompatibility of silk fibroin is needed to be proven as an implantable biomaterial with cell viability and cell proliferation tests. Thus, Live/Dead, and MTT analysis were performed at 1, 7, and 14 days of incubation of hAD-MSCs on scaffolds. Live/Dead images showed that density of the viable cells were increased as time passed. Moreover, the percentage of cell proliferation of hAD-MSCs on the day of 1, 7, and 14 days were found as 90 %, 118 % and 138 %, respectively. This finding showed that the silk fibroin scaffolds can support cell proliferation and viability.

In conclusion, this study showed that fabricated silk fibroin scaffolds are biodegradable, biocompatible systems to be used in cardiac tissue engineering. Despite hAD-MSCs are not common cell source for cardiac therapies, it can be an alternative source for future studies since its isolation, characterization and differentiation was happened as expected. The combination of silk fibroin scaffolds with hAD-MSCs can be a promising approach for future studies.

İNSAN MEZENKİMAL KÖK HÜCRELERİNİN 3B İPEK FİBROİN YAPI İSKELELERİNE UYGULANARAK KARDİYAK DOKU MÜHENDİSLİĞİNDE KULLANILMASI

ÖZET

Ölüm nedenleri arasında kardiyovasküler hastalıklar tüm dünya sıralamasında birinci sıradadır. Kardiyovasküler hastalıklar arasında ise en sıklıkla rastlanan ölüm sebebi kalp krizidir (% 40,5). Kalp krizi sonrası kardiyak hücreler hasar görür ve kendilerini yenileme özelliği olmadığından, bu durum kalp fonksiyonlarında kalıcı hasara neden olur. Bu klinik probleme çözüm bulmak amacı ile β-blokerler, ACE-inhibitörleri, AT1-reseptör blockerleri gibi pek çok farmasötik ilaç kullanılmaktadır. Hastalığın son evresinde ise organ transplantasyonu dışında başka kalıcı bir tedavi yöntemi bulunamamıştır. Bir tıbbi müdahale olarak geçen organ naklinde ise uygun donor bulmak oldukça zordur ve hastanın nakil sonrasında kısa veya uzun vadede organı reddetme olasılığı vardır.

Miyokardiyal enfarktüs, daha bilindik adıyla kalp krizi, koroner arterlerde meydana gelen tıkanıklık sonucu kalp kasının ilgili bölümünün oksijensiz kalması ve bunun sonucunda şiddetli göğüs ağrısıyla ortaya çıkan hastalık durumudur. Kalp miyoblast, fibroblast, hücre dışı matris gibi yapılardan oluşmaktadır. Kas hücrelerinin fazlalığı, oksijen miktarındaki düşüklükleri tolere edemeyebilir, bu da kalp krizinin gerçekleştiği kas dokusunda hücre ölümüne neden olur. Kalp hücreleri tam farklılaşmış hücreler olduğundan kendisini yenileme özelliği bulunmamaktadır. Her beş ani ölümden birinin kalp krizi olduğu ve kalp krizinin hastanelere getirdiği ekonomik yük gerçeği ile kalp krizi için doku mühendisliği yaklaşımları umut vadedici araştırma alanıdır. Kardiyak doku mühendisliği yaklaşımı ile temel olarak hastanın kendi kök hücresini 3 boyutlu iskele yapılar ile bir araya getirerek hasarlı dokuyu tedavi etmek amaçlanmaktadır.

Bu çalışmada insan adipoz dokusundan elde edilen mezenkimal kök hücrelerin doğal ve biyobozunur bir polimer olan ipek fibroinden hazırlanmış 3 boyutlu iskelelere ekilerek *in vitro* koşullarda kardiyak rejenerasyonu amaçlanmıştır. Öncelikle, ipek kozasının içerisindeki serisin proteini uzaklaştırılarak, fibroin proteininin izolasyonu sağlanmıştır. Sonrasında, dondurarak kurutma yöntemi ile üç boyutlu iskele yapılar oluşturulmuştur. Farklı dondurma derecelerinin ve yalıtım levhası kullanılmasının gözenek yapısı üzerindeki etkisi incelenmiştir. Dondurarak kurutma sonrasında metanol işlemi ile fibroin yapısındaki tesadüfi kıvrımların beta-tabaka formuna dönüşmesi sağlanmıştır. Beta-tabaka oluşumunun sağlanması ile daha gözenekli, çözünmesi zor ve kararlı bir yapı elde edilmiştir. Doku iskelelerin karakterizasyonu için morfoloji (taramalı elektron mikroskopu), biyobozunurluk ve su tutma kapasitesi testleri tamamlanmıştır. Değişik ipek fibroin konsantrasyonları (% 1'den % 6'ya) test edilerek, en iyi gözenek yapısına sahip olan iki konsantrasyon (% 2 ve % 4) yalıtım levhası ve metanol etkisinin gözlemlenmesi için seçilmiştir. Dondurma aşamasında yalıtım levhası kullanılması ve ardından metanol işlemi ile, 2 % ve 4 % örnekleri taramalı elektron mikroskopu ile incelenmiştir. Tek yönlü soğutma ve beta-tabaka

yapısının artırılmasının gözenek yapısı üzerindeki etkisi belirgin bir şekilde görülmüştür. Su tutma kapasitesini analiz etmek için 2 % ve 4 % örnekler ile devam edilmiştir. Test sonuçlarında silk fibroinin % 1000 gibi yüksek oranlarda su tutma kapasitesine sahip bir polimer olduğu bulunmuştur, ve sonraki deneylerde yapı bütünlüğünün bozulmaması için daha düşük yüzdede su tutma kapasitesine sahip olan (% 4) ipek fibroin iskele yapısı seçilmiştir. Literatürde ipek fibroin proteini için en yüksek bozunurluğu sağlayan proteaz IV enzimi seçilmiştir. Biyobozunurluk hızı 0.1 U/mL proteaz IV enzimi varlığında 14 günlük süre içinde takip edilmiştir. Sonuçlar ipek fibroinin % 50 ağırlığının ilk 10 gün içerisinde bozunduğunu, ve 14. güne kadar bozunmanın daha yavaş hızda devam ettiğini göstermiştir. Ayrıca, ipek fibroinin enzimsiz PBS varlığında inkübasyonu sonucunda, yaklaşık olarak % 25 ağırlık kaybı gözlemlenmiştir. Sonuçlar enzim aktivitesinin biyobozunurlukta önemli bir yol olduğunu doğrulamıştır.

Çalışmanın ikinci kısmında, Medeniyet Üniversitesi Göztepe Eğitim ve Araştırma Hastanesinden alınan etik kurul raporuna uygun olarak, 40 ve 50 yaş aralığında kadın hastalardan liposuction operasyon sonrası elde edilen yağlardan mezenkimal kök hücreler izole edilmiştir. Adipoz doku, doku mühendisliğinde sıklıkla tercih edilen bir hücre kaynağı olmasa da, tek bir operasyonda fazla sayıda ve kolaylıkla elde edilmesi, birden fazla hücreye farklılaşabilmesi nedeni ile seçilmiştir. Ayrıca kemik iliğinden ve embriyodan alınan kök hücrelere göre etik kaygılar daha azdır. Adipoz dokudan elde edilen mezenkimal kök hücrelerin karakterizasyonu akış sitometri ve immunohistokimya yöntemleri ile yapılmıştır. Akış sitometri yöntemi öncesinde, literatürde ve Uluslararası Kök Hücre Kurumu tarafından belirtilmiş olan mezenkimal kök hücre belirteçlerine göre, izole edilen hücreler CD44, Anti-human-CD166, CD73, CD105, CD90, CD13, CD45, Anti-HLA-DR, CD15, CD34, CD19, CD11b, CD 14, CD45 karakterize edilmiştir. Akış sitometri ile, adipoz dokudan izole edilen hücreler yüksek saflıkta, % 90' ın üzerinde mezenkimal kök hücre olarak karakterize edilmiştir. İkincil kriter olarak, kök hücrelerin üç farklı hücre tipine dönüşmesi potansiyeli test edilmiştir. İmmunohistokimya analizinde adipoz dokudan alınan mezenkimal kök hücrelerin farklı boyama teknikleri ile adiposit, kondrosit ve osteositlere dönüştüğü gösterilmiştir. Kök hücreler sırası ile 14, 21, 21 gün farklılaşma ortamında kültür edildikten sonra, kondrosit, osteosit ve adiposit hücrelere dönüştüğü gözlemlenmiştir. Farklılaşmanın karakterizasyonu için kondrojenik hücrelerde Alcian Blue boya, osteojenik hücrelerde Alizerin Red boya ve adipojenik hücrelerde Oil red O boyası kullanılmış ve anlamlı boyama elde edilmiştir. Daha sonra, mezenkimal kök hücre olarak karakterize edilen hücrelere bir gün süre ile 5-azacytidine, 20 gün süre ile ise geliştirilmiş kardiyak farklılaştırma kültür ortamı sağlanmıştır. Hücrelerin morfolojisinde değişim görülse de, kardiyomiyosit benzeri yapılar görülmemiş ve kardiyak özel belirteçler ile anlamlı boyama sonucu elde edilememiştir. Kardiyomiyosit hücrelere farklılaştırma sürecinin ikinci adımında PSC kardiyomiyosit farklılaşma kiti kullanılmış ve kardiyomiyositlere dönüşüm gerçekleşmiştir. 10 günlük inkübasyon sonunda sarkomerik ve top şeklinde yapılar mikroskopla gözlemlenmiş, α-actinin, Troponin I, Connexin 43 ve Myosin ağır zincir kardiyak belirteçleri ile pozitif boyanmıştır.

Doğal polimer olan ipek fibroinin biyouyumluluğuna ve hücre canlılığına etkisi, MTT, WST-1 ve Live/Dead testleri ile incelenmiştir. Hücre çoğalması kolorimetrik bir yöntem olan MTT testi ile ölçülmüştür. Sonuçlara göre, hücre sayısında 1. günden 14. güne doğru artış gözlemlenmiş, ipek fibroin iskele yapı üzerinde hücre canlılığı 1., 7., ve 14. günlerde sırası ile % 90, % 118 ve % 138 olarak belirlenmiştir.

Bu sonuçlar bize, hazırlanan ipek fibroin iskelelerin güvenilir, biyobozunur bir biyomateryal olarak doku mühendisliği uygulamalarında kullanılabileceğini kanıtlamıştır. Standart bir tıbbi cihaz biyouyumluluk testi olarak WST-1 direkt ve indirekt testleri uygulanmıştır. Her iki test sonucunda, ipek fibroinin kontrol grubuna göre hücre çoğalması sırası ile % 92 ve % 104 bulunmuştur.

Özetle, ipek fibroin kardiyak doku mühendisliği uygulamalarında biyobozunur, biyouyumlu ve çekme direnci özelliklerinden dolayı tercih edilebilir bir biyomateryal olduğu bulunmuştur. Ayrıca, adipoz dokunun izolasyonu, karakterizasyonu ve farklılaştırılmasının sağlanması kardiyak uygulamalarda alternatif hücre kaynağı olarak kullanılabileceğini göstermiştir. Adipoz dokudan elde edilen kök hücrelerin kardiyak hücrelere dönüştürülerek bağışıklık tepkisi yaratmayan biyobozunur ve biyouyumlu 3 boyutlu iskele yapı oluşturulması gelecekteki çalışmalar için umut vericidir. Bunlara ek olarak, adipoz dokudan gelen mezenkimal kök hücreler kardiyomiyosit hücreler ile birlikte kültür edilebilir. Ayrıca, ipek fibroin iskele yapısı başka doğal veya sentetik polimerlerle komposit yapı oluşturarak geliştirilebilir. Elde edilen 3 boyutlu iskele yapı gerçek doku ortamına benzeyen biyoreaktörde test edilebilir. Sonuç olarak, kardiyak farklılaşmanın tam anlamıyla sağlanabilmesi ve biyouyumlu komposit yapıyla test edilmesi için daha kapsamlı çalışma gerekmektedir.

1. INTRODUCTION

1.1 Aim of The Study

Organ or tissue defects is a major health problem in the world. Tissue engineering is a field that combines life sciences, biomaterials science and biomedical engineering approaches to replace or repair damaged organ or tissue after an injury, accident or other damages. Synthetic or naturally derived engineered biomaterials are used to replace damaged or defective tissues such as cartilage, bone, skin etc. These biomaterials are designed as three-dimensional (3D) constructs, called scaffolds which enables cell growth on them to replace implanted scaffolds with new tissue.

Biocompatibility, biodegradation, non-immunogenicity, good biological and mechanical support for cell growth are important parameters for the fabrication of 3D scaffolds. Porous, biodegradable and biocompatible scaffolds promote cell attachment, proliferation, and differentiation with ideal microenvironments. In addition, optimal cell source and biological molecules such as growth factors should be incorporated into scaffolds to improve microenvironment necessary for complete tissue development. Each of three major components; scaffolds, bioactive molecules and cells have significant effect on the result of any study in tissue engineering.

In the current study, silk fibroin from Bombyx mori as a natural, biocompatible and biodegradable polymer was used to construct 3D silk scaffolds for cardiac tissue regeneration. Different concentrations of silk fibroin scaffolds were subjected to SEM, water-uptake, and biodegradation analysis to characterize and compare 3D silk scaffolds.

As a second parameter in the study, human adipose-derived mesenchymal stem cells (hAD-MSCs) were chosen to differentiate into human cardiomyocytes. Physical characterization of hAD-MSCs by flow cytometry, and multi-differentiation potency were tested before cardiac differentiation process. Cardiomyocyte differentiation from hAD-MSCs was performed, and confirmed by cardiac specific markers to prove alternative potency of adipose derived stem cells for cardiac therapies. Cell

viability and cell proliferation tests of hAD-MSCs on 3D silk scaffolds were applied to understand the biocompatibility feature of silk fibroin.

1.2 Clinical Relevance - Cardiovascular Diseases

Millions of people die each year due to cardiovascular diseases in the world. In Turkey, cardiovascular diseases are the leading cause of death (40,3 %) in 2015 (TÜİK). Moreover, the highest rate among deaths caused by cardiovascular diseases was ischemic heart disease (40,5 %) which increases the rate of getting myocardial infarction (TÜİK).

Myocardial Infarction (MI) can cause loss of cardiomyocytes that leads to organ failure or trigger hypertrophy of the healthy myocardium later on. It is known that adult cardiomyocytes have extremely low regenerative capacity, this damage becomes permanent in many patients.

In general, heart failure treatments focus on the protection from catecholamines (β-blockers), angiotensin (ACE-inhibitors, AT1-receptor blockers), and aldosterone (spironolactone). At later stage, the only effective treatment is heart transplantation for good long-term results. (Miniati and Robbins, 2002). However, there are some limitations in heart transplantation for many patients such as limited numbers of appropriate donors and complications after transplantation.

The number of patients with heart failure is increasing despite of surgical and pharmacological treatments,. To overcome this clinical problem which affects millions of people in the world, scientists have been focused on alternative therapeutic strategies to deal with heart failures such as cardiac tissue engineering and cell therapy to regenerate heart function. These drawbacks have led to the relentless research into better ways to deliver stem cells or angiogenic factors (which mobilize stem cells) to the regions of interest to facilitate increased retention, survival, engraftment, and regeneration.

1.3 Myocardial Infarction and Repair

The mammalian heart is a complex muscular pump which has two primary functions such as collecting blood from the other parts of the body and pump it to the lungs,

and collecting fresh blood from the lungs and pump it to all other organs and tissues in the body.

The heart tissue is highly differentiated, so it cannot regenerate after an injury (Pasumarthi and Field, 2002). The heart wall is composed of tightly packed myocytes, fibroblasts, endothelial cells, smooth muscle cells and supporting collagen-based extracellular matrix (ECM) (Severs, 2000). Because of the high density and high metabolic demand of myocytes, their oxygen consumption is very high. Thus, heart cannot tolerate hypoxia.

Acute MI occurs when blood supply to the heart is decreased into a critical level which leads to failure in myocardial cellular repair mechanisms, and failure in homeostasis (Bolooki and Askari, 2010). If coronary artery blood flow sorption continues for more than 20 minutes after acute MI, cell damage and death occur (Figure 1.1).

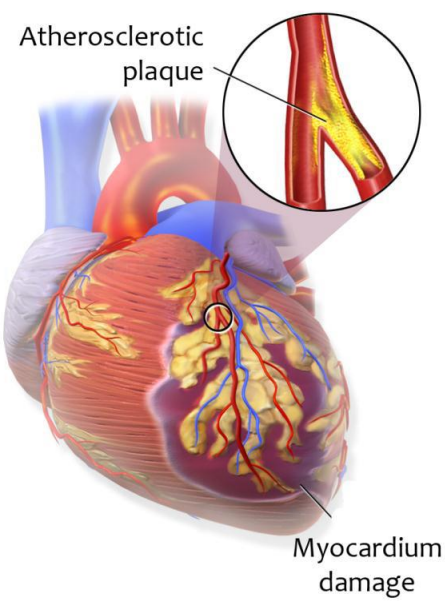

Figure 1.1 : Schematic representation of the MI. Atherosclerotic plaque slowly grows in the inner lining of a coronary artery and causes catastrophic thrombus formation after MI. At the end, it prevents blood flow downstream (Bolooki and Askari, 2010).

After myocardial infarction, inflammatory response take place in scar tissue. Macrophages remove dead cells, fibroblasts and endothelial cells migrate into that area, and forms thick and collagenous scar. Formation of the granulation tissue is not good for the contractile function of the heart, and leads to heart failure after ventricle remodeling (Sun et al., 2002; Nian et al., 2004). Thus, tissue engineering

approaches should aim to reconstruct the scar tissue, and to restore heart function in adults.

The definite therapy for treating MI patients was not found. Therefore, there is a great interest for alternative therapeutic strategies to overcome this disease. These strategies mostly focus on three key approaches; i) direct transplantation of healthy cells such as fetal cardiomyocytes, skeletal myoblasts, and bone marrow stem cells into injured myocardium, ii) development of the replacement tissue by tissue engineering approaches such as using progenitor or stem cells, and iii) development of therapies to promote heart to regenerate scar tissue (Askari et al., 2003).

1.4 Cardiac Tissue Engineering

The aim of tissue engineering is to replace or repair damaged organ or tissue by combining different methods such as delivering healthy cells into damaged tissue, using scaffolds as a biomaterial or biologically active molecules. It combines life sciences and principle of engineering to improve or restore organ function. There have been many attempts in synthesizing structurally similar, healthy tissues such as cartilage, bone, bladder or skin (Vacanti and Langer, 1999).

As a classical tissue engineering approach, specific cells are isolated from the patient with a biopsy, and isolated cells are grown on a three-dimensional (3D) scaffold under controlled conditions. Then, cell-scaffold construct is delivered to the injured site of the same patient to assist new tissue formation with the degradation of scaffold over time (Vacanti and Langer, 1999). Based on this concept, three key elements should be considered; i) a scaffold with good mechanical and biological support for cell growth and differentiation, ii) progenitor cells that can be differentiated into desired cell types, and iii) growth factors/chemicals that regulate cellular activities and differentiation (Leor et al., 2005).

Cardiac tissue engineering strategies can be collected under two titles as in vitro and in vivo approaches (Figure 1.2). In vitro strategies include construction of engineered grafts which is a combination of scaffolds, biomaterial gels or sheets with the cells such as cardiomyocytes, fibroblasts, or smooth muscle cells in a bioreactor or culture dish. In vivo tissue engineering strategies can be cell transplantation, implantation of cell seeded or unseeded scaffolds, injection of scaffolds with or without cells, and delivery of active molecules to promote healing or self-repair. In both strategies,

there are some advantages and drawbacks. In in-vitro approaches, it is easier to control scaffold size, shape, cell development and function, but the ability to form a strong muscle, and the risks of tissue necrosis restricted after transplantation to patient's body. On the other hand, *in vivo* approach aims to replace injured tissue in natural environment. It is more feasible than *in vitro* approach, but controling the development of engineered graft and prediction of its consequences are limited (Leor et al., 2005).

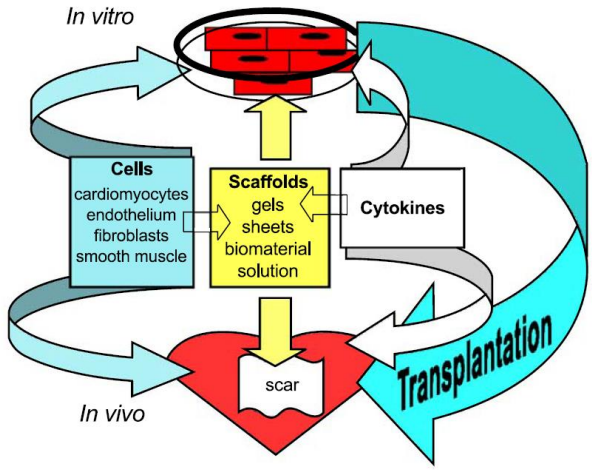

Figure 1.2 : Strategies of tissue engineering can be collected under two title as in vitro and in vivo approaches (Leor et al., 2005).

Worldwide increase in CVD resulted in urgent need to improve treatments to prevent heart disease. One of the solutions might be in vitro engineering of 3D scaffold according to the patient's need before implantation. At the very beginning of this approach, cardiomyocytes embedded in a mixture of type I collagen gel and matrigel were used to improve left ventricular function after MI. Thus, implantation of engineered tissue has been proven to treat CVDs (Zimmermann et al., 2006). Later, multiple materials including collagen gels, chitosan foams, polyglycolic acid meshes, fibrin glues, and polyethylene glycol (PEG) hydrogels have been tested for cardiac tissue engineering (Rinaldi, 2014). Combination of relevant cells with these scaffolds can be suitable strategy for implantation on damaged site, but it has drawbacks too. Collagen gels and foams have been characterized by mechanical weakness and random microstructures which would lead undesired microenvironment even if they could promote a differentiated cardiac muscle (Feng et al., 2003; Akhyari et al., 2002). Moreover, collagen gels have an isotropic morphology that minimizes cellular attachment and requires external stimulator factors to induce alignment such as

electrical stimulation or mechanical stretch (Costa et al., 2003; Akhyari et al., 2002; Radisic et al., 2004).

To achieve directed cell growth, several strategies have been applied. Poly (glycolic acid) (PLGA) membranes by electrospinning technique, for example, have ability to mimic fibril structure of the heart extracellular matrix, and vascularized ventricular myocardial tissue. However, the constructing appropriate thickness of PLGA membrane and the high degradation rate are challenging because the scaffold can collapse easily (Chen et al., 2008).

There has not been perfect biomaterial that could mimic all important characteristics of the myocardium. Recent research has been focused on the use of natural environment of heart decellularized with sodium dodecyl sulfate (SDS) and repopulated (Ott et al., 2008). Although, functional 3D cardiac tissue was obtained, high mechanical stiffness was observed due to SDS treatment or ECM compaction. Thus, a new tunable biomaterial approach is needed which should focus on mimicking native structural, mechanical and transport properties to create a biomimetic cardiac construct.

For the regeneration of 3D cardiac tissue, a biodegradable scaffold should be fabricated that mimics in vivo ECM, and provides cell attachment, migration, growth and function properly on injured tissue (Wang et al., 2006). Schematic steps of tissue engineering are shown in Figure 1.3. Various natural and synthetic materials such as collagen, hyaluronan, chitosan, cellulose, and mulberry silk have been tested for 3D cardiac tissue patches (Willerth and Sakiyama-Elbert, 2008). Production of synthetic materials is easy and cheap, but their degradation can cause inflammatory response, and mostly toxic (Laflamme and Murry, 2011). On the other hand, natural materials are degradable based on metabolic processes, but they may also cause an immunogenic response in host which results in implant rejection. Among natural biomaterials, silk fibroin protein has unique mechanical strength, and biocompatibility. Besides that, fabrication of silk fibroin into different morphologies is relatively easy (Omenetto and Kaplan, 2010; Talukdar et al., 2011). Moreover, it has non-cytotoxic property and cause relatively low inflammatory response. Thus, the characteristics of silk fibroin as mentioned above make it an excellent biomaterial for use in tissue engineering.

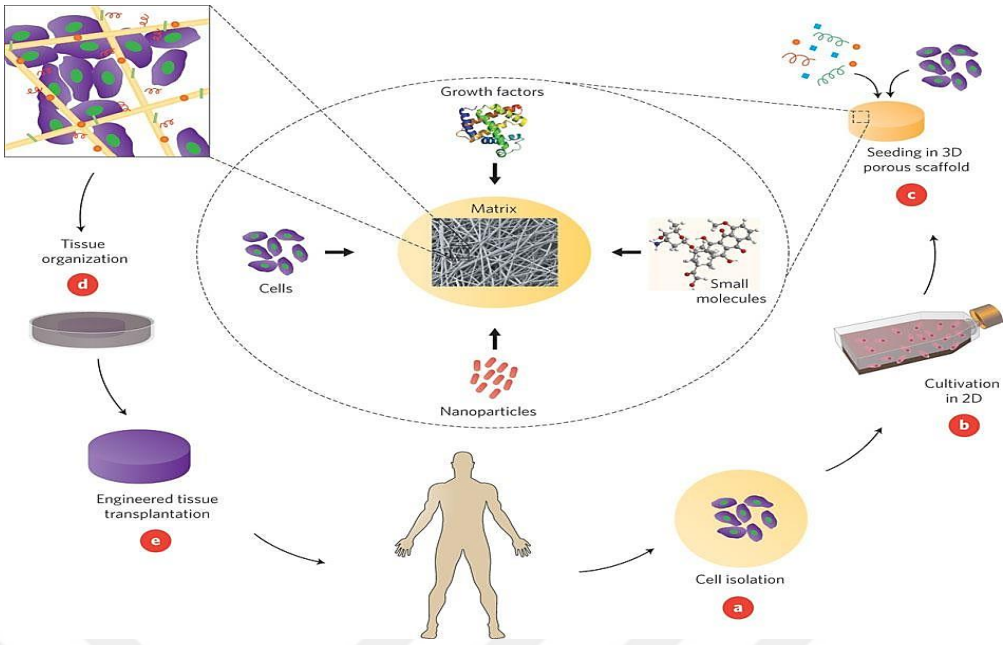

Figure 1.3 : Schematic steps of tissue engineering approach (Dvir et al., 2011).

1.5 Silk as a Biomaterial

Silks are fibrous proteins that are produced by spiders, silkworms, or other insects (Motta et al., 2002). Silkworm silk from Bombyx mori is used as a biomaterial for many different applications, and it has two main protein components; 70-80 % fibroin, and 20-30 % sericin in mass (Kim et al., 2005) (Figure 1.4). This natural polymer consists of Glycine and Alanine as the main amino acid residues, and coated with a sericin, a gum-like protein. The pure silk fibroin protein is prepared by degumming procedure, and sericin is removed during purification step to avoid adverse immune response after implantation (Haifeng et al., 2006).

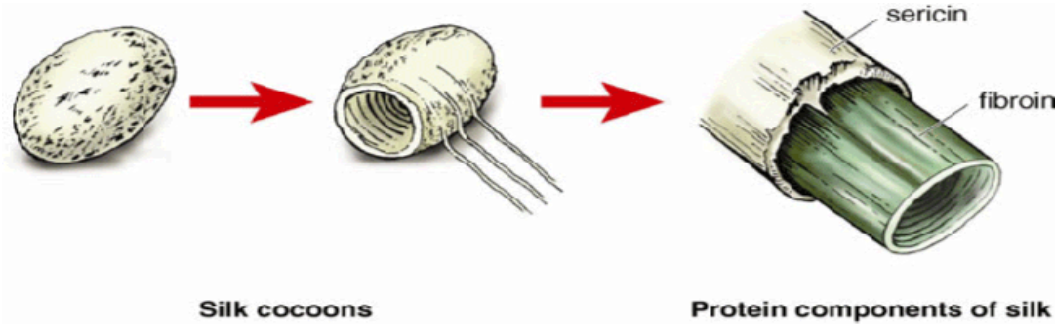

Figure 1.4 : Two main protein components of silk protein; sericin and fibroin (Silk Fibroin, Tes Teach., 2017).

Silk has a large molecular weight (200–350 kDa or more), and is composed of a heavy and a light chain linked together by a disulfide bonds. There are two types of

silk due to variations in hydrophobic and hydrophilic domains of amino acid structure between mulberry and non-mulberry silks, higher or lower basic/acid, polar/non-polar, and bulky/non-bulky. These structural changes cause significant differences in the mechanical properties, bioactivity and the degradation behavior between mulberry and non-mulberry silks (Kundu et al., 2013). As an example, silk fibroin has different ratios of random coil, alpha helix and beta sheet structures which are related with the solubility and exceptional tensile strength feature of the protein. If random coil structure concentration is high, the protein will be more soluble. If the structure of the protein is changed by increasing beta sheet conformation with treatments such as methanol, the protein will be insoluble (Jin et al., 2005).

Silk fibroin has been studied extensively due to its favorable biological responses (Meinel et al., 2005). It has been used in textile for centuries. In recent years, silk fibroin is used in medical and tissue engineering applications due to its many advantages over other biopolymers with the features of high tensile strength, biocompatibility, flexibility, lower inflammatory potential and controlled biodegradation (Perez et al., 2001).

1.5.1 Silk fibroin fabrication technique

There are various fabrication methods developed in the last decade to construct 3D biomimetic scaffolds for tissue engineering such as gas foaming, electrospinning, phase-separation, freeze drying, rapid-prototyping and self-assembly (Lu et al., 2013) (Table 1.1). Different silk structures such as electrospun fibers, sponges, microspheres, hydrogels and films can be processed with the techniques as mentioned below (Jones et al., 2009) (Figure 1.5). To obtain desirable features of silk solution, some aspects like porosity, interconnectivity, degradation, mechanical strength etc. must be evaluated because of providing suitable microenvironment for cell-attachment and proliferation on scaffolds (Liu and Peter, 2003).

Table 1.1 : 3D fabrication technologies of polymer scaffolds (Chen et al., 2008).

Fabrication Technology	Required properties of materials	Available pore size (μm)	Porosity (%)	Porous Structure
Melting-based				
Melt moulding	Thermoplastic	50-500	<80	Spherical pores/low interconnectivity
Extrusion/particle leaching	Thermoplastic	<100	<84	Spherical pores/low interconnectivity
Solvent-based				
Solvent casting	Soluble	30-300	20-50	Irregular pores
Paraffin template	Soluble	100-700	>90 %	Spherical pores
Emulsion freeze-drying	Soluble	<200	<97	High volume of interconnected micropores
Freeze drying	Soluble	<200	<97	High volume of interconnected micropores
Electrospinning	Soluble	20-100	<95	Fibrous
Membrane lamination	Soluble	30-300	<85	Irregular pores
Gas foaming				
Chemical reactant gas foaming	Amorphous	100-700	>90 %	High volume of non-interconnected micropores
Physical induced gas foaming	Amorphous	Micropores <50	< 97	Low volume of non-interconnected microporescombined with high volume of interconnected micropores
Rapid Prototping				
3D Printing	Soluble		<70	100 % interconnected macrospores
Fused deposition remodeling				
Direct rapid prototyping				

Among different fabrication techniques, freeze drying, also known as lyophilization is a drying process for converting solutions into solids of enough stability for distribution or storage. It has been also widely used to prepare porous materials for tissue engineering. Leaching of particles, emulsion templating, phase separation, three-dimensional printing and electrochemistry are the other techniques to prepare porous materials. These processes require large amount of organic solvent usage or etching procedure. However, water, environmentally friendly solvent, is used in freeze drying. Removing water from the solution does not also cause impurities in sample. Thus, additional purifying process is not necessary (Qian and Zhang, 2010). Moreover, various fibroin sponges can be obtained with different freezing conditions.

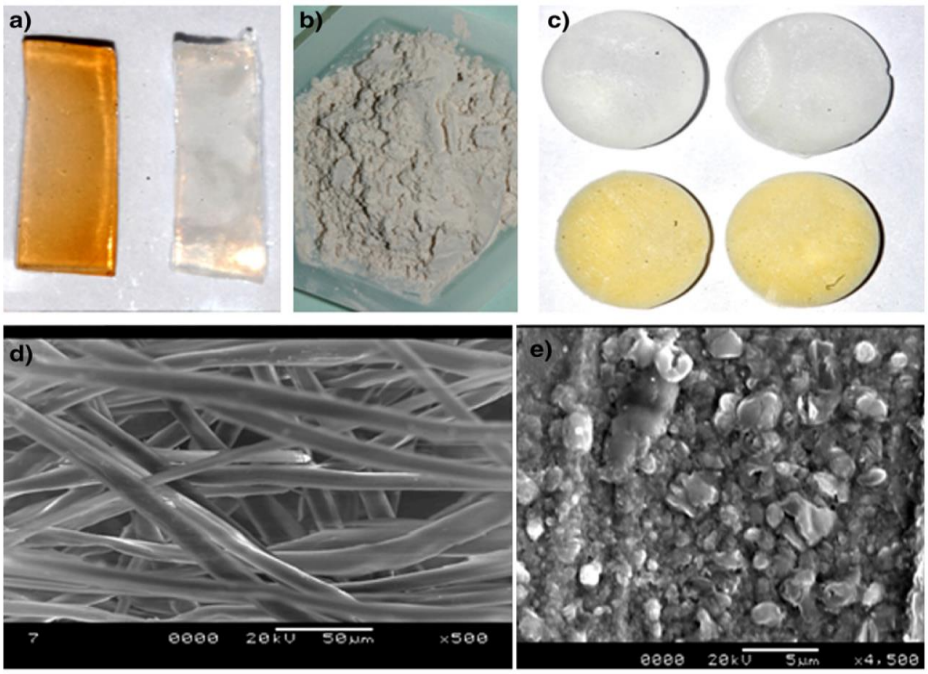

Figure 1.5 : Schematic representation of biomaterials fabricated from silk fibroin: (a) hydrogels; (b) lyophilized powder; (c) 3D porous scaffolds; (d) native silk mat; (e) silk microparticles (Kundu et al., 2013).

Freeze-drying process includes three major steps; freezing, primary drying, and secondary drying. At the beginning, the solution is frozen at low temperature (−20°C to −80°C). Then, frozen sample is located in a chamber where the pressure is lowered through a vacuum. This step is called as primary drying process where ice in the material is removed by sublimation. In secondary drying process, most of the unfrozen water in the material is removed by desorption (Lu et al., 2013).

For the fabrication of 3D porous scaffolds, freeze-drying method has been widely used in last two decades. As an example, methacrylamide-modified gelatin-2-hydroxyethyl methacrylate porous scaffolds were fabricated by this method, and the human foreskin fibroblasts were seeded onto these scaffolds with high (95%) viability after 7 days culture. Moreover, porous polysaccharide-based scaffolds were prepared with different pore diameter (55–243 μm) and porosity (33%–68%) with the regulation of freeze-drying parameters (Lu et al., 2013). Seeding of human mesenchymal stem cells on both porous and non-porous polysaccharide-based scaffolds was also experimented. Pore sizes of the freeze-dried sponges can be adjusted by changing freezing temperature, pH of the solution and the amount of organic solvent., and repeating freezing and thawing processes can increase the pore sizes up to 250 μm according to the study of Kundu et al. (2013). As an alternative to

freeze-drying process, solvent casting/particle leaching or gas-foaming methods have better control over pore structure, especially in bone and cartilage tissue engineering applications (Meinel et al., 2005).

1.5.2 3D silk sponge for tissue engineering approaches

3D porous sponges are suitable biomaterials for tissue engineering applications, because they can mimic the in-vivo microenvironment around the target tissues. 3D silk sponges or silk scaffolds can be prepared by freeze drying, porogen leaching and solid free form fabrication techniques (Li et al., 2001). To obtain better mechanical and biological results, silk can be prepared by organic or inorganic fillers to make composite silk scaffolds. However, the compatibility between different components can be challenging because sustaining homogenous distribution in scaffold design is important. If compatibility of composite material is poor, it results in phase separation and adverse tissue reactions. To overcome this issue and to obtain good compatibility, some modifications such as improvement in compressive modulus or reinforcement with fine silk fibers to obtain improvement in modulus can be done (Hokugo et al., 2006). As an example for the improvement, silk composites reinforced with knitted silk mesh were used as a ligament scaffold without using any metal support for bone regeneration, and uniform distribution of cells after implantation was found out (Fan et al., 2008).

Moreover, chitosan or hyaluronic acid loaded silk fibroin scaffolds seeded with rat mesenchymal stem cells were used to form cardiac patches (Kundu et al., 2013). In another study, silk fibroin 3-D scaffolds from A. mylitta showed good results in producing beating rat cardiomyocytes in-vitro (Kundu et al., 2013). Cardiomyocytes were attached to 2D fibronectin coated silk film, which improved metabolic activity as compared to gelatin coated scaffolds. Since it is known that anisotropic alignment is important for cell attachment and proliferation, a simple freeze-drying process can provide available pore sizes to the silk. Even though there are some critical issues need to be resolved, silk has a good potential for cardiac tissue engineering, because of its mechanical strength, biocompatibility, and ease of modifying stiffness and porosity of the product. Moreover, it has relatively straightforward process to construct long term culture in vitro and integration in vivo (Kundu et al., 2013).

1.6 Cell Sources for Cardiac Tissue Engineering

In cardiac tissue engineering applications, choosing optimal cell source is one of the important key parameters. The optimal cell source should be easily harvested, nonimmunogenic, be able to proliferate and/or differentiate into functional cardiomyocytes. However, there is no such a cell source for ideal cardiac tissue engineering therapy. A variety of cell sources have been isolated and used to repair the injured cardiac tissue mostly in animal models, but only limited percentage ends up on clinical trials (Chen et al., 2008). The potential cell sources for myocardial regeneration in human, and their advantages/disadvantages are shown in Table 1.2.

Table 1.2 : Advantages and disadvantages of potential cell sources for cardiac tissue engineering (Chen et al., 2008).

	Cell Source	Autologous	Easily Obtainable	Highly Expandable	Cardiac Myogenesis	Clinical Trial	Safety
Somatic Cells	Foetal Cardiomyocytes	No	No	No	Yes	No	No
	Skeletal Myoblasts	Yes	Yes	Depend on Age	Debated	Yes	Yes, arrhythmias
	Smooth Muscle Cells	Yes	Yes	Yes	No	No	No
	Fibroblasts	Yes	Yes	Yes	No	No	No
Somatic Stem Cells	Mesenchymal Stem Cells	Yes	No	Depend on Age	Yes	No	Yes, fibrosis calcification
	Endothelial Progenitor Cells	Yes	Yes	Depend on Age	Debated	No	Yes, calcification
	Crude Bone Marrow	Yes	Yes	Depend on Age	Debated	Yes	Yes, calcification
	Umbilical Cord Cells	No	Yes	Yes	Debated	No	No
	Adipose Stem Cells	Yes	Yes	Yes	Yes	No	Yes
Embryonic Stem Cells	Human Embryonic Stem Cells	No	No	Yes	Yes	No	Yes, potential teratoma if cells escape differentiation

A variety of cell types has been under investigation to repair and improve injured cardiac cells' function (Figure 1.6). They can be categorized under three cell types:

i) somatic muscle cells, such as skeletal myoblasts, fetal or natal cardiomyocytes ii) myocardium-generating stem cells, such as embryonic and bone marrow/adipose-derived stem cells, iii) angiogenesis-stimulating cells, such as fibroblasts and endothelial progenitor cells (Chen et al., 2008).

Each cell type has advantages and disadvantages to be used in cardiac tissue engineering approaches. While allogenic cells are relatively easy to obtain compared to autologous cells, they can cause immunosuppression. Autologous cells do not cause immune response, but they are more difficult to obtain (Leor et al., 2005). Natal or foenatal cardiomyocytes can be an ideal cell type because of their natural electrophysiological, structural, and contractile properties, but cardiomyocytes are difficult to isolate, expand, and can also cause immune response in host tissue. The most common used cell types for cardiac tissue engineering are skeletal muscle-derived progenitors, and crude bone marrow mononuclear cells (Lee and Makkar, 2004). However, the limitation of skeletal muscle-derived progenitors is their inability to differentiate into cardiac or endothelial cells.

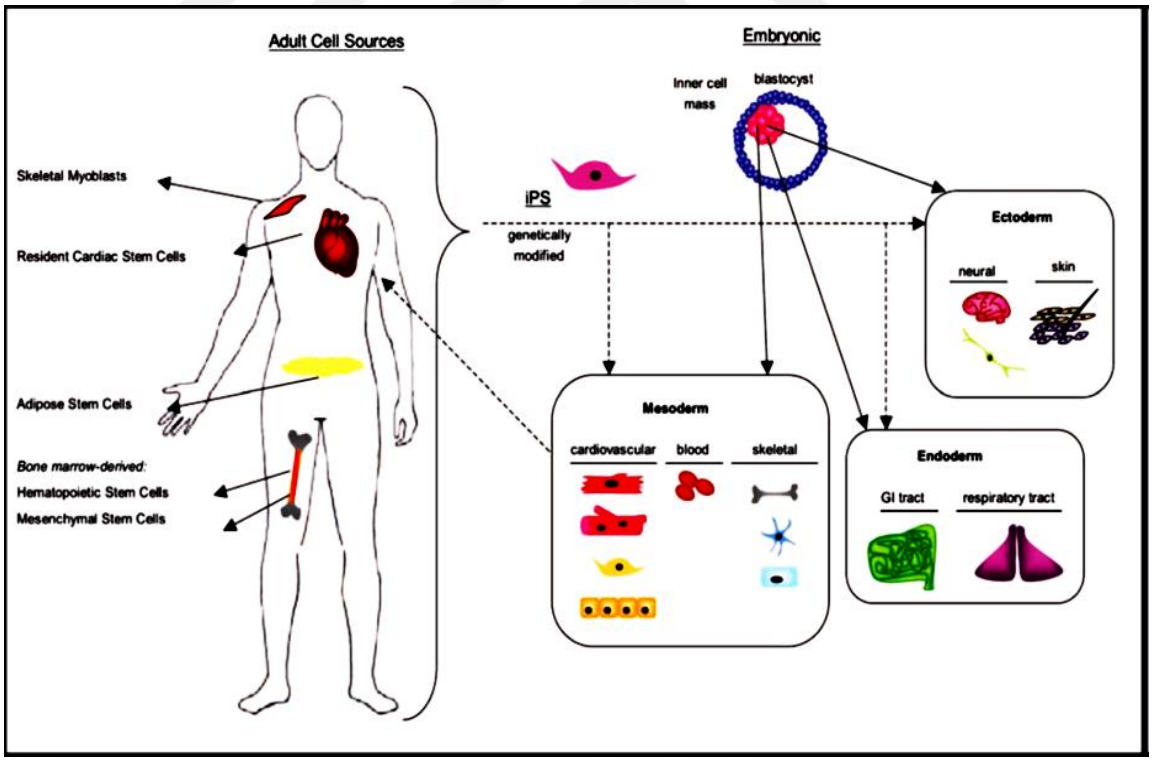

Figure 1.6 : Potential cell sources for cardiac tissue engineering (Vunjak-Novakovic et al., 2010).

Furthermore, there are some safety concerns concerning the usage of various cells for cardiac therapy. Arrhythmias were seen with skeletal myoblasts (Smits et al., 2003).

Moreover, cardiac calcifications with bone-marrow mononuclear cells (Yoon et al., 2004), myocardial scarring with mesenchymal stem cells (Vulliet et al., 2004), and teratoma with human embryonic stem cells are common concerns reported in the literature (Thomson et al., 1998).

In summary, the suitable cell source for cardiac repair has still needed further investigation and optimization. Our study focuses on mesenchymal stem cell-based approach in combination with biomaterial which has good mechanical strength, biocompatibility, ease of modifying stiffness and porosity for regeneration of injured cardiac tissue.

1.6.1 Stem cells

The stem cells are undifferentiated cells that have two common characteristics: i) ability to renew themselves, or proliferate indefinitely, ii) potential to differentiate into more than one specialized cell types (Alison et al., 2002). Throughout their cell life, they have capacity of self-replication with unlimited numbers. Moreover, each stem cell can form a colony with identical genetic constitution. Because of their characteristics as mentioned above, stem cells are optimal cell source for tissue engineering, and many researches on cardiac muscle regeneration has been done during last decade (Leor et al., 2008).

According to their differentiation potentials, stem cells can be categorized into two types: i) pluripotent stem cells (PSCs; including embryonic stem cells (ESCs) and induced pluripotent stem cells (iPSCs)), ii) adult stem cells. Pluripotent stem cells can generate hundreds of cell types that form the adult body. However, adult stem cells can only differentiate into specialized mature cells. According to their potency, stem cells can be categorized as totipotent, pluripotent, multipotent, and unipotent as shown in Figure 1.7.

In addition to categorization in terms of potency of stem cells, there are five sources for stem cells. Adult stem cells are mostly multipotent cells which are found in undifferentiated cells of a specific tissue. They can present in all tissues and survive under harsh conditions. Embryonic stem cells can be obtained from undifferentiated inner cell mass of an early stage of embryo, and it can be described as both totipotent and pluripotent. They can differentiate into more than 200 cell types. Foetal stem cells are obtained from the very early development stage of the foetus, and they are

also described as pluripotent. Cord blood stem cells are obtained from the blood of the placenta and umblical cord after birth, and are also multipotent stem cells. Lastly, cancer stem cells, malignant transformation of adult stem cells, can be a source for the stem cells (Vats et al., 2002).

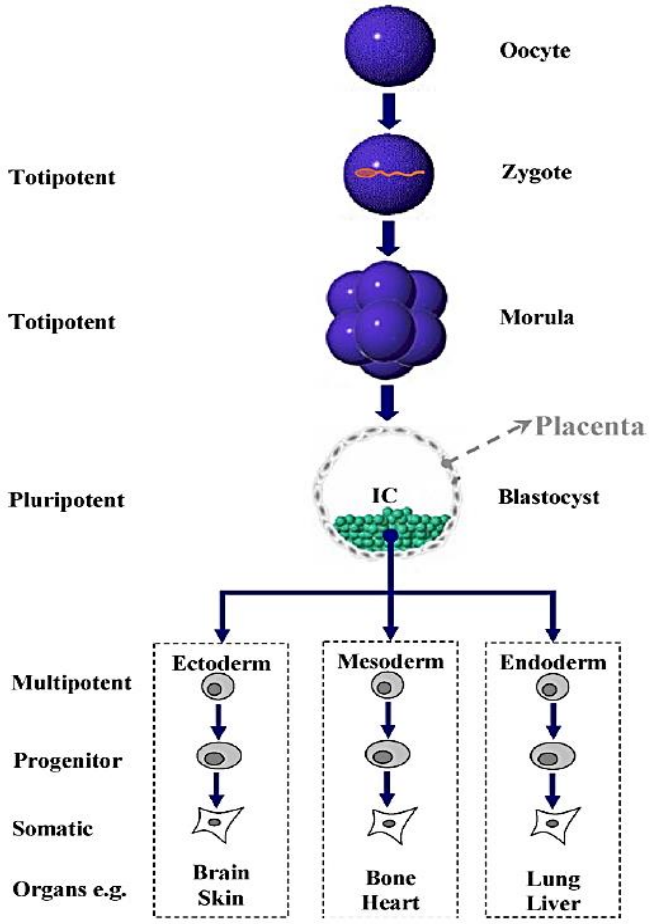

Figure 1.7 : Categories of stem cells in terms of potency (Chen et al., 2008).

In this study, adipose-derived adult stem cells were used as a cell source for cardiac tissue engineering. Thus, human adipose derived mesenchymal stem cells are going to be our main focus among the other stem cell types.

1.6.2 Human adipose-derived mesenchymal stem cells

Adipose derived mesenchymal stem cells (AD-MSCs) have the ability to differentiate into multiple cell types. However, their differentiation potential is more limited, and maintaining and expansion of these cells in vitro is difficult compared to pluripotent stem cells. Adipose tissue consists of mature adipocytes, stromal vascular

fraction, and subpopulation of the multipotential stem cells. It is isolated from a variety of sources, including human white and brown adipose tissues (Mazo et al., 2011). Human adipose tissue provides abundant and relatively easy accessible source for adult stem cells used in various tissue engineering applications.

Similar to other mesenchymal stem cells, such as bone marrow-derived or cardiac progenitor cells, AD-MSCs have ability to differentiate into osteogenic, chondrogenic, and adipogenic cell types. The advantages of AD-MSCs for cardiac cell therapies are relatively easy isolation and ability of long-term expansion in vitro. There are limited ethical issues with AD-MSCs, and they have ability to generate autologous therapies as an advantage.

There are several studies reported on the differentiation of adipose derived stem cells into cardiomyocytes. Animal trials with rats showed that the implantation of AD-MSCs improved heart function after MI (Chen et al., 2008). In the study of Planat-Bénard et al. (2004), the use of 5-azacytidine as a stimulator factor for differentiation of AD-MSCs was induced the expression of cardiac specific markers such as GATA4, NKX2.5, ANP, MLC2v, and MLC2. In addition, the existence of functional atrial, ventricular, and nodal cardiomyocytes were shown by ultrastructural and electrophysiological analyses. In some studies conducted in animal models with cardiac damage, including direct intramyocardial injection or indirect injections to deliver ADMSCs through intravenous or intracoronary resulted in repair of damaged myocardial tissue (Chen et al., 2008). A clinical trial can be given as an example for the improvement of heart function by the injection of AD-MSCs in patients with ischemic myocardium. The transendocardial injections of AD-MSCs showed significant improvements in total left ventricular mass and reduction in ischemia (Chen et al., 2008). These studies proved that, AD-MSCs improved ventricular function, myocardial perfusion, and exercise capacity in patients with ischemia.

Even though these studies are not sufficient enough, it is challenging to obtain cardiomyocytes from AD-MSCs which are easy to harvest in large numbers compared to bone marrow-derived stem cells (BM-MSCs). Moreover, they have similar properties and differentiation potential as BMMSCs which is a widely used adult stem cell source (Zuk et al., 2001, 2002). Thus, AD-MSCs can be a good alternative for cardiac cell therapies.

2. MATERIALS AND METHODS

This study consists of two parts; i) development of silk fibroin scaffold and its characterization: ii) the characterization of isolated human adipose-derived mesenchymal stem cells (hAD-MSCs) and their application on silk fibroin scaffolds. First, optimization for the production process of silk fibroin scaffolds were carried out, and the best percentage of silk fibroin to use as a biomaterial was determined for the cell culture studies according to SEM analysis results. Then, its water uptake and biodegradation capacity were identified.

In the second part, the isolation and then characterization of hAD-MSCs were performed. The biocompatibility of silk fibroin scaffolds on hAD-MSCs, was investigated by 3-(4,5-Dimethylthiazol-2-Yl)-2,5-Diphenyltetrazolium Bromide (MTT), Water Soluble Tetrazolium Salts-1 (WST-1) and live/death assays. The cardiomyocyte differentiation potential of hAD-MSCs was investigated by immunofluorescence staining of cardiac biomarkers.

2.1 Materials and Laboratory Equipment

2.1.1 Chemical and materials

The chemical and materials that were used in the laboratory with their supplier companies are listed in Appendix A.

2.1.2 Laboratory equipment

The list of equipments in the laboratory is given with their supplier companies in Appendix B.

2.1.3 Solutions

The solutions that were used in this study and their compositions are given in Appendix C.

2.2 Method

2.2.1 Fibroin extraction from Bombyx mori silkworm cocoons

Bombyx mori silkworm cocoons were supplied from Kozabirlik (Bursa). Silk fibroin extraction and purification were performed as described by Rockwood et al., (2011). Briefly, silkworm cocoons were cut into pieces until 5 gram silk cocoons obtained. The ultrapure water (2 Liters) was heated up to boiling point, then 0.02M Na_2CO3 was added to the boiled water. When sodium carbonate (Na_2CO3) was completely dissolved, the 5 gram of silk cocoons was added to the solution to remove sericin protein. After 30 minutes, the silk fibroin was squeezed to remove the excess water, and washed with ultrapure water. After that, the silk fibroin was rinsed in ultrapure water and the water was changed after an hour. This step was repeated for three times. Finally, silk fibroin was removed from the water, squeezed well, then spread out on a clean aluminum foil. The silk fibroin was allowed to dry in a fume hood for overnight.

On the next day, the dried silk fibroin was dissolved at 60 ℃ in 9.3 M lithium bromide solution (LiBr) which is a strong solvent that breaks disulphide bonds in fibroin to prepare a final concentration of 20 w/v % LiBr-Silk fibroin. The resulted viscous, amber colour solution was inserted into previously hydrated dialysis cassette (3500 Molecular Weight Cut off) with 20 mL syringe. The solution was dialyzed against 1 L of ultrapure water for each cassette. The water was refreshed 6 times for 48 hours. A large stir bar was used to mix the solution during dialysis.

After 2 days, the silk fibroin was removed from both cassettes, and split into 15 mL conical tubes before centrifugation step. The aqueous solution was centrifuged at 9,000 rpm and 4 ^{o}C for 20 minutes. This step was repeated 2 or 3 times depending on the impurities that were seen in the tubes. In each step of purification, the silk was transferred into a new conical tube. Finally, 0.5 mL of the silk fibroin solution was weighted (*Wwt*), and dried in an oven at 6^{o}C overnight to determine the concentration of the silk fibroin. Dried silk fibroin was calculated as *Wdry*. The yield was calculated according to Equation 2.1.

$$\text{Yield (\%)} = (\underline{Wdry - Wwt}) / Wwt \text{ X } 100 \quad (2.1)$$

At the end, the silk solution was diluted into 1%, 2 %, 3%, 4 %, 5%, 6 % (w/v) to construct different fibroin samples in terms of surface morphology and porosity. Main steps in silk fibroin extraction process were showed in Figure 2.1.

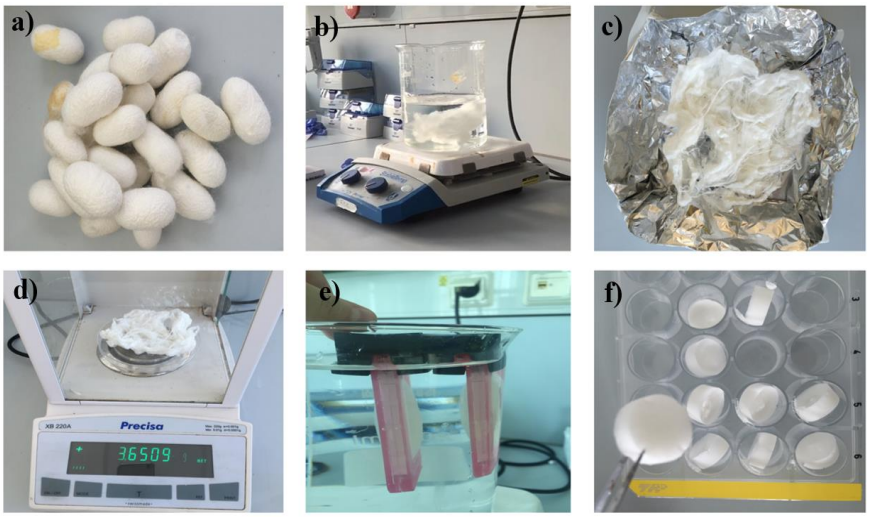

Figure 2.1: Main steps of fibroin extraction from Bombyx mori silkworm cocoons (a-d; extraction before LiBr, e; dialysis of silk fibroin, f; silk fibroin scaffolds after liyophilization step).

2.2.2 Lyophilization of silk fibroin solutions

The silk fibroin solution was poured on 24-well plate (1 mL silk fibroin solution/well) and the top of the well plate was covered with styrofoam to provide unidirectional cooling in -20 °C refrigerator and left overnight before lyophilization step.

On the next day, the frozen silk solution was lyophilized in a freeze-dryer (Figure 2.1(f)). To main drying step, the parameters of freeze-dryer were set up to - 30 °C for 24 hours, and then set up to - 20 °C for 1 hour for the final drying.

Methanol Treatment

After lyophilization process, water-insoluble polymer was treated with methanol to induce β-sheet formation. First, the weight of silk fibroin polymer in the each well was calculated to determine the amount of methanol needed. Since it is known that 1 mL of methanol is enough for 1.7 g of silk fibroin, the amount of methanol was calculated according to the percentage of silk fibroin (2 % and 4 %) in the scaffold. The freeze-dried samples were treated with 97 % of methanol in a vacuum hood for

half an hour (Chomchalao et al., 2013). After this step, samples can be stored at room temperature for years.

2.2.3 Characterization of silk fibroin scaffolds

2.2.3.1 Analysis with scanning electron microscopy

Scanning Electron Microscope (SEM) was used to analyze the surface morphology and the porosity of silk fibroin scaffolds. Scaffolds were cut into two pieces to get the picture of inner sectionsi and the surface morphology was analyzed at 25x, 70x, and 250x magnification.

2.2.3.2 Water-uptake test of silk fibroin scaffolds

The water-uptake capacity of 2 %, and 4% silk fibroin scaffolds was tested according to the protocol developed by Lerdchai et. al (2016). Phosphate buffered saline (PBS) solution (0.01 M, pH 7.4) was used to determine water uptake capacity of each scaffold. Before the test, dry samples were weighted (*Wdry*), and then incubated with PBS at 37 ºC for 24 hours. The excess PBS solution was removed by pipette up, and swollen samples were weighted (*Wwet*). According to Equation 2.2, the water uptake capacity of samples was calculated in percentage. For each type of silk fibroin scaffold, the samples were used in triplicate and the results were presented as average.

$$\text{Water uptake ratio (\%)} = [(Wwet - Wdry) / Wdry] \text{ X } 100 \qquad (2.2)$$

2.2.3.3 Biodegradation test of silk fibroin scaffolds

For the biodegradation process, PBS containing Protease XIV (from Streptomyces griseus with 3.5 units/mg) was used for the degradation of 2 %, and 4 % silk scaffolds. Enzyme concentration (0.1 U/mL) was calculated based on a study conducted by Lu et al., (2009).

Since the degradation studies were carried out at 37ºC, scaffolds might be prone to the microbial growth. To prevent this problem, sodium azide was added to both enzyme containing and enzyme-free PBS solution at a ratio of 0.01% (w/v) (Lerdchai et. al., 2016).

Before the test, the dry samples were weighed (Wi) and then placed into 24-well plates. Protease XIV (1 mL, 0.1 U/mL) enzyme solution was added to the

each sample except control samples, and samples were remained on a shaker at 37 ℃, 30 rpm for different time intervals of 3, 7, 10, and 14 days.

Solutions in both sample and control wells were refreshed every 2 days to provide continuous enzymatic activity. At 3, 7, 10, and 14 days, samples were taken out, excess amount of solution was removed, and rinsed in distilled water. Scaffolds were then weighted (Wf), and the percentage of remaining sample weight was calculated according to the Equation 2.3. Also, the average of 2 %, and 4 % silk scaffolds for each week was calculated.

$$\text{Remaining weight ratio (\%)} = [(Wi - Wf) / Wi] \times 100 \quad (2.3)$$

2.2.4 Isolation and characterization of mesenchymal stem cells

2.2.4.1 Isolation of MSCs from human adipose tissue

Human (woman age between 40 and 50 years) subcutaneous adipose tissue was freshly taken from the patient who was under anesthesia during liposuction process with the approval of the Istanbul Medeniyet University, Goztepe Training and Research Hospital Ethics Committee. The patients were aware of the post-operation procedure for this study, and signed a paper about being informed.

In each liposuction operation, approximately 300 ml fat was obtained under sterile conditions, and they were freshly kept on ice until the isolation procedure starts. The time between the isolation procedure and operation is critical, thus isolation must be started as soon as possible according to the procedure as described by Francis et al., (2010).

First, 300 ml of fat was divided into 50 ml falcon tubes. In each tube, 25 ml of PBS suplemented 100 I.U./ml penicillin, 100 µg/ml streptomycin and 2.50 µg/ml amphotericin B and 25 ml of fat was mixed, and centrifuged at 400 g for 5 minutes. After centrifugation, the lower phase was discarded, and oil phase was washed 3 to 5 times with PBS until the solution becomes clear. Then, 0.01 % type I and type II collagenase in equal amounts were prepared to add on fat solution (0,045 g collagenase I and 0,045 g collagenase II in 45 ml PBS). The solution with collagenase enzyme was incubated in a shaker at 120 rpm 37℃ for 2 hours. After, the solution became like orange juice, DMEM medium was

added on the solution to inhibit collagenase activity with Fetal Bovine Serum (FBS). Then, the solution was centrifuged at 800 g for 10 minutes. Floating adipocytes and liquids was aspirated. The Stromal Vascular Fraction (SVF) was resuspended in 160 mM NH_4Cl for 10 minutes at room temperature to burst erythrocytes which were discarded by centrifuge at 400 g for 10 minutes. The pellet was resuspended in PBS, and filtered through 70 µM nylon mesh. The passed cells were centrifuged again at 400 g for 10 minutes, and resuspended in DMEM supplemented with 10% FBS, 1% antibiotic/antimycotic solution, 1% non-essential amino acids and 1% glutamax, then cultured on 150 mL flasks. Flasks were incubated overnight at 37 ℃ and 5% CO_2. After incubation, flasks were washed with PBS to remove residual non-adherent cells, and the medium was refreshed 3 times a week.

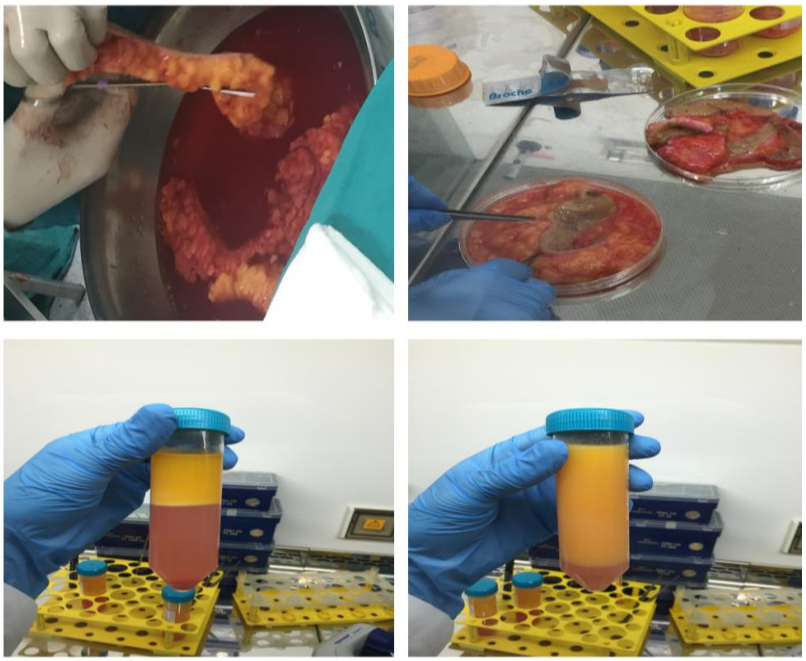

Figure 2.2: Images of Isolation Procedure of Human Adipose-Derived Mesenchymal Stem Cells.

2.2.4.2 Expansion of hAD-MSCs

When the hAD-MSCs reached 80 % confluence, they were subcultured. The medium in 150 flasks was aspirated and the cells were washed with 10 mL PBS. Then, PBS was aspirated from the flasks without touching hAD-MSCs. Trypsin-Ethylenediaminetetraaceticacid (EDTA) (0.25%) in 2.5 mL was added into the flask, and incubated at 37 ℃ for 5 minutes to detach cells. Later, 5 mL

of DMEM was added, and the hAD-MSCs were harvested by pipette up and down. The cell suspention was transferred into the 50 mL tube, and centrifuged at 1500 rpm for 8 minutes. The supernatant was aspirated and the cells were resuspended in DMEM, then the cell number was calculated with hemocytometer under the inverted microscope. The hAD-MSCs were used for characterization and differentiation experiments at the passage number 3.

2.2.4.3 Characterization of mesenchymal stem cells

Phenotype characterization of hAD-MSCs

In literature, the minimum criteria for the MSCs surface phenotyping is expression of CD105, CD73 and CD90 (human MSC-positive cellular markers and genes) accompanied by the lock of expression of CD34, CD45, CD14 or CD11b and HLA-DR (human MSC-negative cellular markers and genes) (Dominici et al., 2006). The isolated and expanded hAD-MSCs at passage number 3 were stained with required antibodies to measure the percentage of positive and negative cell surface markers.

The Flow cytometry analysis of hAD-MSC specific markers such as CD44, CD73, CD13, CD90, CD166, CD105, CD13 (positive cellular markers), and CD11b, CD34, CD15, CD14, CD19, CD45, anti HLA-DR (negative cellular markers) was performed by Stem Cell and Gene Therapy R&D Center, Kocaeli University.

Determining multi-differentiation potential

Human MSCs (hMSCs) are the non-haematopoietic, multipotent stem cells with the capacity to differentiate into mesodermal lineage such as osteocytes, adipocytes and chondrocytes, etc. Multilineage potential, immunomodulation and secretion of anti-inflammatory molecules makes MSCs an effective tool in the treatment of chronic diseases. Therefore, in this study isolated MSCs needed to be characterized to evaluate multi-differentiation potential into osteocytes, adipocytes and chondrocytes (Zuk et al., 2002).

Osteocyte differentiation of hAD-MSCs

Osteogenic differentiation kit was purchased from StemPro®. hAD-MSCs were harvested when their confluency was reached to 60-80 %. The hAD-

MSCs at passage 3 was seeded at a cell density of $5x10^3$ cells/well on coverglasses in the 24-well plate. The cells in growth medium was incubated at 37 ºC and 5% CO_2 for 2 days.

The differentiation medium of hAD-MSCs was added and incubated for at least 21 days at 37°C, 5% CO_2). During that period of time, hAD-MSCs were refeeded every 2 or 3 days.

The osteogenic differentiation marker, osteocalcin was detected by Alizarin Red staining. (Cheng et al., 2011). After 21th day, the medium was removed, and the hAD-MSCs were rinsed once with DPBS. Then, hAD-MSCs were fixed with % 4 formaldehyde for 30 minutes. After fixation, hAD-MSCs were washed twice with distilled water, and stained with 2 % Alizarin Red S solution (pH 4.2) at room temperature for 10 minutes incubation. Then, hAD-MSCs were rinsed three times with distilled water. Finally, the differentiation marker of osteogenic lineages, osteocalcin was observed under a light microscope.

Chondrocyte Differentiation of hAD-MSCs

Chondrogenic differentiation kit was purchased from StemPro®, and the given protocol by StemPro® was followed. The hAD-MSCs was harvested when they reached 60-80 % confluency at passage number 3. To examine chondrogenic differentiation, hAD-MSCs was seeded in both form as a monolayer at seeding cell density of 5 x 10^3 cells on coverglasses and as a micromass at seeding cell density of 2×10^5 cells/well into the 24-well plate. Before adding Chondrogenesis Differentiation Medium, the micromass cultures were incubated for 2 hours to provide attachment of the cells. Then, chondrogenic medium was warmed up to 37ºC and added into monolayer and micromass forms into the 24-well plate. The differentiation mediumm was reshed every 2-3 days for 14 days.

After at least 14 days of differentiating time, the medium was removed from each well, and the cultures were rinsed once with DPBS. The hAD-MSCs were fixed with 4 % formaldehyde solution for 30 minutes. Then, both the monolayer and micromass were stained with 1% Alcian Blue solution prepared in 0.1 N HCL for 30 minutes. Finally, they were rinsed three times with 0.1 N

HCl, and the distilled water was added to neutralize the acidity. After staining, the hAD-MSC differentiation into chondrogenic lineage was analyzed under light microscope and development of blue staining indicates the synthesis of proteoglycans by chondrocytes.

Adipocyte Differentiation of hAD-MSCs

Adipogenic Differentiation Medium was purchased from StemPro®. hAD-MSCs were harvested at passage number 3 and seeded at a cell density of $5x10^3$ per well into 24-well plate and incubated in DMEM medium until they reached 80 % of confluency. Then, DMEM medium was aspirated, and replaced with complete MesenCult™ Adipogenic Differentiation Medium. The cells were incubated at 37ºC and 5% CO_2 and the medium was changed every 2-3 days. During the differentiation process which takes 10 - 20 days, the formation of lipid vacuoles was easily observed by Oil Red O staining.

After 21 days, the cells were carefully washed with Dulbecco's PBS, w/o Ca++/ Mg++, and the fixative solution, neutral buffered formalin (10%) to cover the cell monolayer was added. Then, the fixed cells were incubated at room temperature for at least 30 min. Oil Red O (0.3 %) was prepared in isopropanol as a stock solution. On the day of experiment, Oil Red O stock solution was diluted to 0.18 % with distilled water and filtered with a syringe filter and used within 30 min. Fixative solution was aspirated, and the wells were rinsed with deionized water twice. Then, 60% of isopropanol was added to cover the cell monolayer, and incubated for 5 minutes at room temperature. After, dehydration solution was removed. Oil Red O Stain Solution (2 mL) was added into the each well, and 24-well plate was incubated at 37°C and 5% CO_2 for 30 minutes. Oil Red O. solution was removed, and the cell monolayer was rinsed with deionized water twice. Finally, 1 mL of PBS was added to each well (Meirelles et al., 2008), and intracellular lipid vesicles in mature adipocytes were visualized intense red under the light microscope.

2.2.4.4 Cardiomyocyte differentiation of hAD-MSCs

Cardiomyocyte differentiation of hAD-MSCs was induced by using two protocols: i) 5-azacytidine (5-AZA) as described by Carvalho et al., (2012); ii) pluripotent stem cells (PSCs) Cardiomyocyte Differentiation Kit as described

by the product protocol. i) For induction of 5-AZA protocol, the hAD-MSCs at passage number 3 was seeded into both the coverglasses and silk fibroin scaffolds into the 24-well plate at a cell density of $5x10^4$ cells/well and 1 mL of DMEM growth medium was added. Following 1-2 days incubation period, DMEM growth medium was aspirated from each well and 5µM 5-AZA in full DMEM medium was added on top of the cells to induce cardiomyocyte differentiation, and it was removed after 24 hours incubation at 37ºC, and 5 % CO_2. After that, the cells were cultured with cardiomyogenic differentiation medium DMEM supplemented with 1.0 ng/ml of FGF2, 5 x 10^{-7} M of dexamethasone, 10 ng/ml of TGF-beta 1, 1% (5 µg/m) of ITS Premix (Insulin-Transferrin-Selenium), 50 µg/ml of L-ascorbate-2-phosphate for 14 days. At the end of the differentiation period, the medium was aspirated, and the cells were washed with PBS twice. Then, immunofloresence assay protocol was followed. ii) PSC Cardiomyocyte Differentiation Kit (ThermoFisher Scientific) was purchased for the cardiac differentiation of hAD-MSCs. This kit includes 3 different medium; Medium A, Medium B, and Cardiomyocyte Maintenance Medium. According to the given protocol by product information, the hAD-MSCs at passage number 3 was seeded into both the coverglasses at a cell density of $1x10^5$ cells, and silk fibroin scaffolds at a cell density of $2x10^5$ cells into the 24-well plate. Then, 1 mL of DMEM growth medium was added, and hAD-MSCs were incubated at 37ºC, and 5 % CO_2 for 2 days.

First, DMEM was removed, and Medium A (800 µL for scaffolds, 500 uL for MSCs) was added on the hAD-MSCs, and incubated for 2 days. After, Medium A was removed, and Medium B (800 µL for scaffolds, 500 µL for MSCs) was added on the cells, and incubated for 3 days. Then, Medium B was removed and the maintenance medium was added on the cells until the 10th day of differentiation period. In all experiments, each study was performed in triplicate. As a control, the hAD-MSCs at the same cell density on the 3 wells/silk fibroin scaffolds in the 24-well plate were incubated with only DMEM growth medium during differentiation period.

At the 10th day of differentiation, the cells on the coverglassess and on the silk fibroin scaffolds were fixed, and stained with specific cardiac markers to characterize the cardiac differentiation by immunofloresence assay.

Immunofluorescence assay

After induction to differentiation, plates were washed with PBS solution and the cells fixed with 4 % paraformaldehyde in phosphate buffer solution for 15 minutes. After that, the cells were washed twice with PBS for 10 minutes and permeabilized with 0.25 % Triton X-100 followed by three washes with PBS only. The coverslips containing treated cells were blocked with 1% bovine serum albumin (BSA) and 5% goat serum in PBS. Then, they were incubated with the primary antibody for 2 hours in a humid chamber at 4ºC. Cardiomyogenic differentiation markers were analyzed by immunofluorescence assay using primary antibodies human anti-sarcomeric-α-actinin (1:25 dilution), and human anti-connexin 43 (1:100 dilution), anti-troponin I (1:200 dilution), anti-myosin heavy chain (1:200 dilution) followed by goat anti-rabbit and goat anti-mouse Alexa 555 fluorochrome (both in a dilution of 1:400) conjugated secondary antibodies. The nucleus was stained with DAPI (0.2 µg/mL). The coverslips were mounted over the slide with the aid of one drop of Hydromount and protected from light. Samples were analyzed using Leica fluorescence microscopy. The cells incubated only with secondary antibody were used as negative controls. Images were viewed and individually captured using 420 to 460 nm (blue), 510 to 560 nm (green), and 560 to 660 nm (red) filters.

2.2.4.5 Biocompatibility of silk fibroin scaffolds and effects on cell viability

MTT assay for cell proliferation

The hAD-MSCs were cultured at a cell density of $1x10^5$ on the silk fibroin scaffolds and into the three empty wells as a control in the 24-well plates, and incubated at 37ºC, and % 5 CO_2 for 1, 7, and 14 days. The medium was changed three times a week. One more silk fibroin scaffold with no cells was used to evaluate the interference with MTT. After 1, 7, and 14 incubation days, the cell monolayer on the scaffolds and on the wells were washed with PBS, and MTT solution (5 µg/ml) was added into each well in the 24 well plates, and incubated at 37°C and 5 % CO2 for at least 4 hours. After incubation, 800 µL DMSO solution was added to solve the formazan crystals and incubated for 24 hours. After a day, 100 µL of solution from each well was transferred into

96-well plate and absorbances were measured at 562 nm using microplate reader.

Biocompatibility of silk fibroin scaffolds by WST-1 assay

To evaluate the effects of biodegradable components on cell viability, biocompatibility of silk fibroin scaffolds was examined by indirect contact and direct contact methods as described by the standards of Biological Evaluation of Medical Devices, ISO 10993-5. i) Indirect contact method: Silk fibroin scaffolds were sterilized under UV light. Each surface was exposured to UV light twice for 30 minutes. Scaffolds were extracted with DMEM at a ratio of 6 cm^2/mL for 72 hours at 37 ^oC, and 120 rpm.

The hAD-MSCs (at passage 4) were seeded at a cell density of $1.5x10^4$ cells/well into the 96-well plate and incubated for 24 hours at 37°C and 5 % CO_2. After that, the 100 µl of extract from silk fibroin scaffolds were added on hAD-MSCs in triplicate. After 24 hours exposure to the extract, WST-1 reagent prepared as 10 % in the DMEM growth medium was added on each sample and control, then incubated at 37 ^oC, and %5 CO_2 for 2 to 4 hours. Then, the absorbance of formazan product was measured at 450 nm by ELISA reader.

ii) Direct contact: The hAD-MSCs was seeded at a cell density of 1x105 on the sterilized scaffolds and on the wells as controls in triplicate in the 24-well plate and incubated at 37 ^oC, and %5 CO_2 for 24 hours. Following day, the medium was aspirated and 10% WST-1 reagent was added into the scaffolds and the control monolayers. After 2-4 hours incubation period, the absorbance of the formazan product was measured at 450 nm by ELISA reader.

Cell viability by Live/Dead Analysis

LIVE/DEAD® Viability/Cytotoxicity Kit from Molecular Probes provides a two-color fluorescence that measure recognized parameters of cell viability-intracellular esterase activity and plasma membrane integrity was used. Calcein AM at excitation – emission wavelengths of 485 – 530 nm generates green fluorescence signal in live cells, and ethidium homodimer (EthD-1) at

excitation – emission wavelengths of 530 – 645 nm generates red fluorescence signal in dead cells.

Each side of silk fibroin scaffolds was exposed to UV light for sterilization for 30 minutes and they were placed into the 24-well plate. Then, 1 mL of growth medium was added on them into the wells. hAD-MSCs at a cell density of $1x10^5$ were added on both scaffolds, and empty wells (as a control). DMEM growth medium in 1 mL was added on each well, then incubated at 37 ^oC, and %5 CO_2 for 1, 7, and 14 days. A silk fibroin scaffold with no cell was used to examine the interference with the WST-1 reagents.

Following incubation period, hAD-MSCs were washed with DPBS solution twice to remove serum esterase activity. LIVE/DEAD reagents were removed from the freezer and warm up to room temperature. Then, 10 mL of working solution including 4 μM of calcein AM, and 4 μM of EthD-1 in DPBS was prepared, and 800 μL solution was added on silk fibroin scaffolds and monolayers. hAD-MSCs were incubated for 1 hours at 37°C, 5% CO_2. After incubation, hAD-MSCs were washed with PBS twice, and immediately observed under the fluorescence microscope.

3. RESULTS AND DISCUSSION

3.1 Characterization of Scaffolds

3.1.1 Morphology of scaffolds

Silk fibroin extraction procedure was completed, and total yield of the silk fibroin solution was found in the range between 5.5 % and 6.8 %. At the beginning of the study, finding the optimum percentage of the silk fibroin in a cardiac scaffold was important. For this, different percentage of silk scaffolds such as 1%, 2%, 3%, 4%, 5%, 6% were produced and characterized with SEM (Figure 3.2). According to the first results, 2 % and 4 % silk scaffolds were chosen for further analysis in terms of their porous structure. Diameter and height of both scaffolds were calculated as 3 x 2.5 cm (Figure 3.1).

Figure 3.1 : Comperative size of 3D Silk Scaffold vs coins.

The concentration of the silk fibroin, freezing temperature and freezing direction effects pore size and distribution (Qian and Zhang, 2010). In a previous MSc thesis study, the effect of an insulation cover during freezing process was tested on composite Poly L-lactide acid and silk fibroin scaffolds and higher porosity was observed after insulation cover (Ozcan, 2016.). Thus, insulation cover was tested for silk fibroin scaffolds in 24-well plate during 24 hours freezing process before lyophilization step. Homogeneous pore distribution was obtained with the help of one directional freezing. Higher pore size and pore distribution after insulation cover were seen clearly with 2% and 4% silk scaffolds (Figure 3.3 and 3.4).

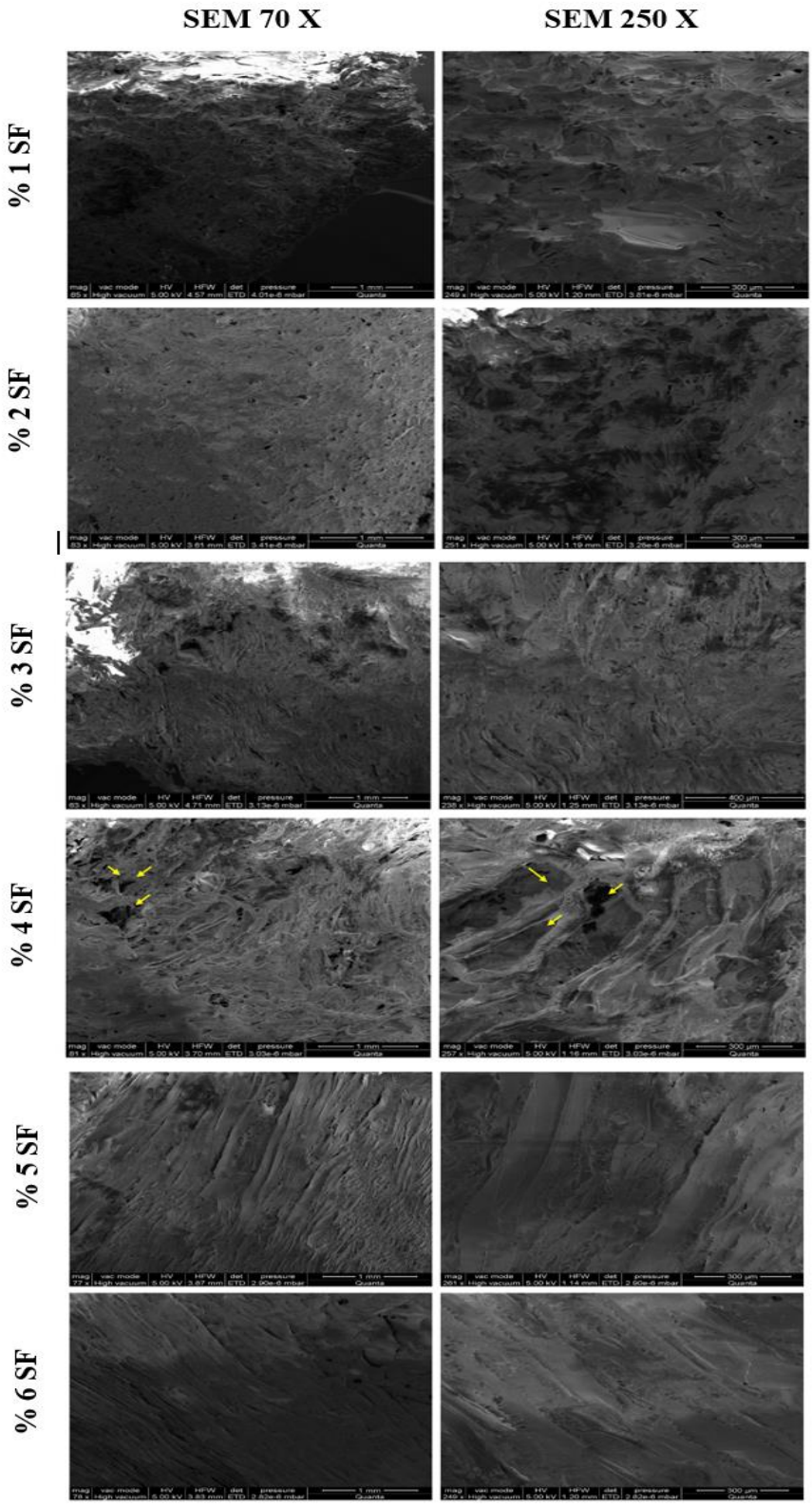

Figure 3.2 : SEM images of SF in order without insulation cover at 70 X and 250 X, respectively 1%, 2%, 3%, 4%, 5%, 6%.

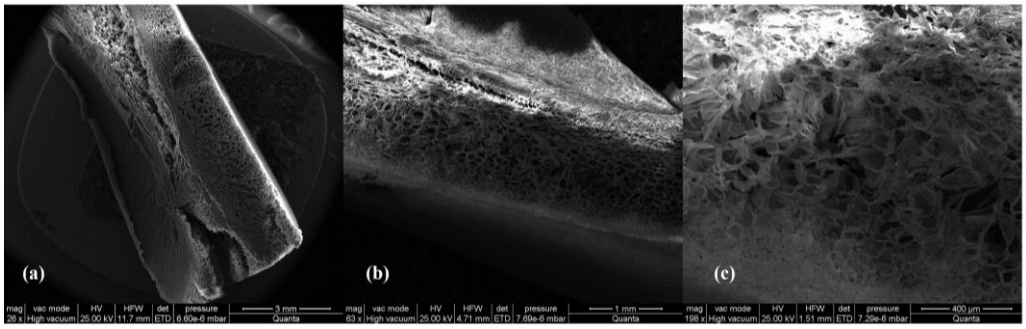

Figure 3.3 : SEM images of 2% SF with insulation cover at (a)25x, (b)65x, (c)180x.

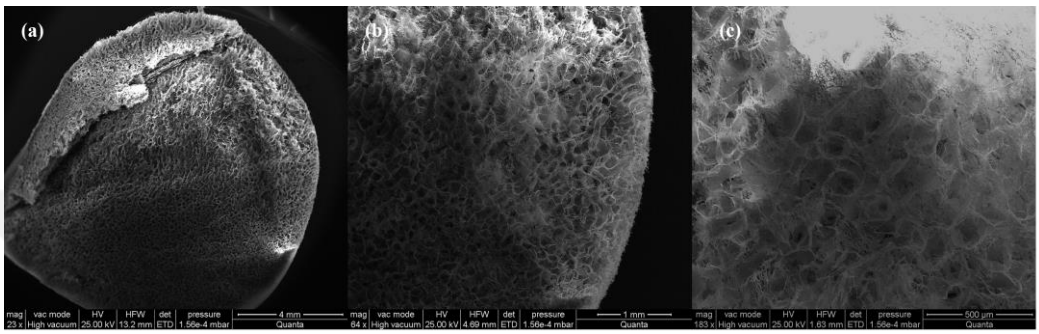

Figure 3.4 : SEM images of 4 % SF with insulation cover at (a)25x, (b)65x, (c)180x.

Higher porosity after insulation cover was a crucial step to continue with those scaffolds for further analysis, because the homogenous pore formation is a significant step that provides the uniform attachment of cardiomyocytes on the wall of the pores. Based on the results, 2 % and 4 % silk scaffolds were chosen for water uptake and biodegradation tests.

3.1.2 Water uptake analysis of silk scaffolds

In tissue engineering, water uptake capacity of a biomaterial is an important property because the scaffold should take fluids from the medium to provide mass transport for the cells (Liang et al., 2010). The capacity of water uptake depends on the polymer composition. In this study, different percentage of silk scaffolds (2 %, 4 %) were tested to compare their water uptake ratios. The results were obtained after 24 hours.

Both scaffolds showed high water uptake capacities (> 1000%). The average of water uptake ratios was approximately 2470 % and 1034 % for 2 % and 4 % silk scaffold respectively after 24h (Figure 3.5). This result showed that both scaffolds have a good fluid uptake capability by maintaining their structural integrity. However, the higher water uptake capacity leads to apparent changes

in size and dimensions of the scaffolds. These results are consistent with the results of the study (Yan et al., 2012), which correlates increased water uptake ratio with decreased silk fibroin concentration.

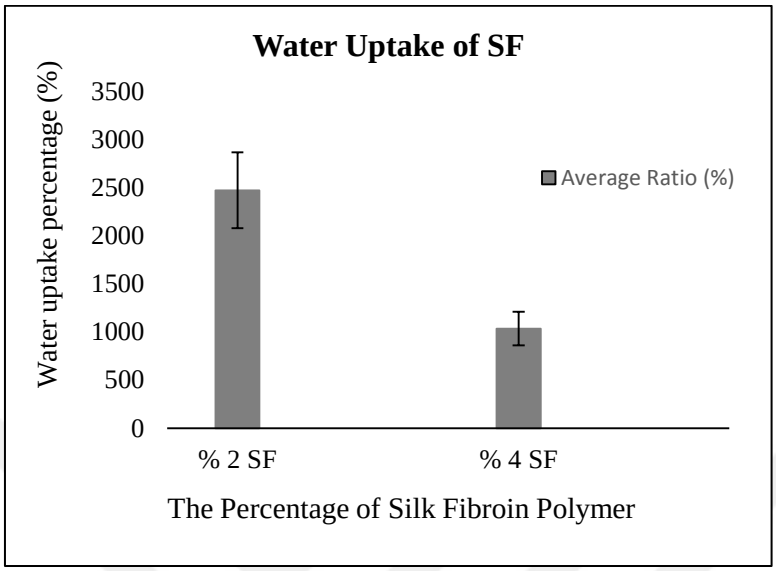

Figure 3.5 : Water uptake behaviour of 2% and 4% scaffolds after 24h.

Due to the structural changes as a result of higher fluid uptake, 4 % silk scaffold which had lower water uptake capacity was chosen for the cell viability and biocompatibility analysis.

3.1.3 Biodegredation analysis of silk fibroin scaffolds

The biodegradability is very important for biomaterials used in tissue engineering. According to the biodegradation protocol described by Brown et al., (2015), 0.1U/mL concentration of protease XIV enzyme was chosen to test degradation rate of silk scaffolds. For control group, enzyme-free PBS was used.

For the degradation of silk fibroin, different kinds of enzymes were tested such as α-chymotrypsin, collagenase IA and protease XIV, protease XXIII, and degradation rates of silk fibroin by different enzymes were compared (Wongnarat and Srihanam, 2013). Significant degradation rates have been found to be obtained by protease XIV enzyme. Protease XIV was compared with α-chymotrypsin, and silk matrix incubated in the Protease XIV significantly decreases while silk matrix in α-chymotrypsin remained unchanged (Cao and Wang, 2009). Moreover, the average molecular weight of

the fibroin samples after degradation with protease XIV, collagenase IA, and a-chymotrypsin was found as protease XIV ≤ collagenase IA ≤ a-chymotrypsin (Li et al., 2003).

Based on this information Protease XIV enzyme was chosen due to its high potency in degradation of silk fibroin. In the first experiment, weight of silk fibroin after degradation was a little bit more than the weight before degradation. It was thought that reason of that can be both from insufficient drying process, and/or microbial growth on scaffolds. Thus, two parameters were changed. First, silk scaffolds were dried for at least 3 hours at 80℃ in drying-oven after biodegradation process was completed. Second, sodium azide was used to prevent microbial contamination on scaffolds.

Silk fibroin scaffolds (4 %) lost almost 50 % of their weight after 3 days of biodegradation in enzyme presence, and showed a slower degradation rate in remaining 10 days. At the end of 14th day, only 26 w% of the scaffolds were remained. It is known that silk fibroin is a biodegradable material, and degradation process varies based on form of silk fibroin. For silk fibroin scaffolds, degradation behavior depends on the isolation method, structural differences such as pore size, silk fibroin concentration (Wang et al., 2008). Even in enzyme-free PBS solution, silk fibroin scaffold lost 74% of its weight after 14 days of biodegradation (Figure 3.6). These results are consistent with the study of Li et al., (2003) which showed that the weight of the silk fibroin sheet was 30 %, and 68 % of its starting weight after 15 days in protease XIV solution and PBS, respectively. Thus, silk fibroin material is a biodegradable material and its degradation rate highly dependent on the protease activity in its environment.

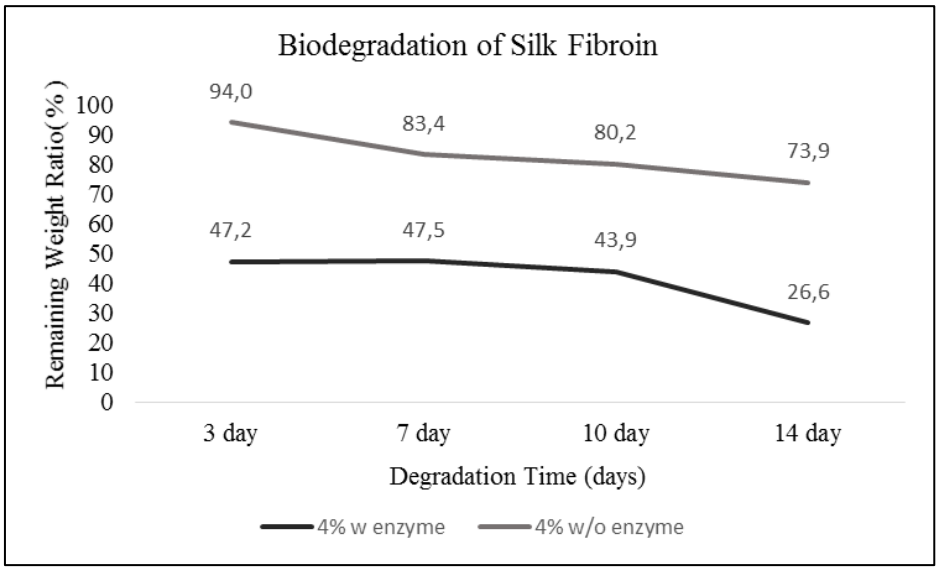

Figure 3.6 : Remaining weight ratio of 4 % scaffold with and without 0.1U/ml protease XIV enzyme in PBS for 14 days.

3.2 MSCs Isolation and Phenotype Characterization

3.2.1 Flow cytometry

The MSCs were isolated from human lipoaspirates by enzymatic and mechanical methods. The heterogenous cell population was cultured in the culture flask and expanded up to passage number 3 to eliminate endothelial, adipocytes, and stromal cells. The adherent cells derived from lipoaspirate expansion had markedly distinct MSCs phenotypic and biological properties. To determine cell surface marker signatures of MSCs that provides a quality control for their successful isolation and for their differentiation potential, flow cytometry was performed for immunophenotyping of isolated MSCs. At the third passage of hAD-MSCs, phenotype of the isolated cells was examined by flow cytometry with investigating specific human cellular surface markers in Stem Cell and Gene Therapy R&D Center, Kocaeli University. The International Society for Cell Therapy (ISCT) has recommended a specific cell surface signature for MSCs. In the literature, MSCs must express CD44, CD90, and CD105, and must lock expression of the endothelial lineage and hematopoietic lineage markers CD31, CD34, and CD45 (Cheng et al., 2011).

In this study, negative cellular surface markers such as CD45, anti-HLA-DR, CD15, CD34, CD19, CD11b, CD 14 and positive cellular surface markers as CD44, anti-human-CD166, CD73, CD105, CD90, CD13 were analyzed by

flow cytometry. The percentage of each cellular surface marker in the isolated hAD-MSCs was given in the Table 3.1. According to the results, the percentage of examined positive markers CD44 (% 99.51), anti-human-CD166 (% 90.25), CD73 (% 91.24), CD105 (% 93.27), CD90 (% 99.11), CD13 (% 89.43) were found higher than 89 % while the percentage of negative markers, CD45, Anti-HLA-DR, CD15, CD34, CD19, CD11b, CD 14 were found less than 1.6 % (Figure 3.7.). These data proved that the phenotype of cells isolated from the human adipose tissue was approximately 90% of mesenchymal stem cells which is sufficient and acceptable phenotypic cells to use for further studies. Moreover, the lack of HLA-DR expression combines with the immunosuppressive properties of hAD-MSCs, and eliminates the risk of tissue rejection due to the suitable allogenic transplantation in clinical use (Cheng et al., 2011).

These results showed that the phenotypic characterization of hAD-MSCs prior to investigate multi-differentiation potential of isolated cells was sufficient for further use. Other cells types found in the isolated cells may be morphologically similar to MSC in vitro such as hematopoietic cells. However, CD45 which stands for hematopoietic cells was found 0.35 % of the isolated cells.

In this study, the surface marker CD90 expressed on MSCs was more than 96, and was not expressed by fibroblast or hematopoietic cells. Therefore, more than 90% of the culture was characterized as MSCs indeed with high level of purity. These results also proved that adipose derived mesenchymal stem cells could be an alternative source for stem cell therapy.

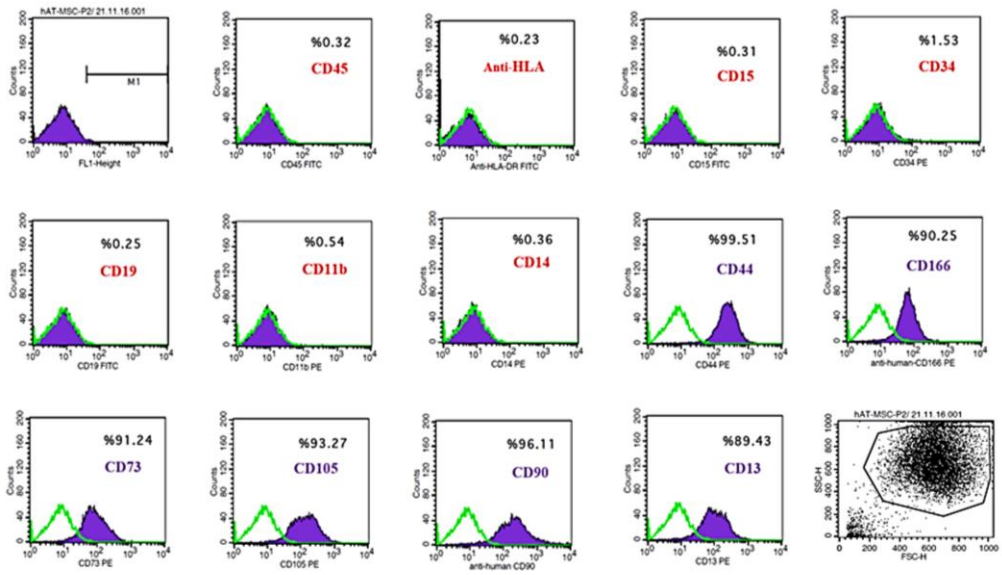

Figure 3.7 : Flow cytometry analysis of human adipose-derived mysenchymal stem cells (hAD-MSCs). The specific cell suface markers of hAD-MSCs at passage number 3 were detected. The specific positive (CD44, Anti-human-CD166, CD73, CD105, CD90, CD13) and negative (CD45, Anti-HLA-DR, CD15, CD34, CD19, CD11b, CD 14, CD34, and CD45) cell suface antibodies on the hAD-MSCs were stained and anayzed by BD FACS Calibur (BD Biosciences).

Table 3.1 : Percentage of positive and negative cell surface markers of hAD-MSCs as a result of flow characterization.

Negative Markers	Percentage (%)	Positive Markers	Percentage (%)
CD45	0.32	CD44	99.51
Anti-HLA-DR	0.23	Anti-human-CD166	90.25
CD15	0.31	CD73	91.24
CD34	1.53	CD105	93.27
CD19	0.25	CD90	96.11
CD11b	0.54	CD13	89.43
CD 14	0.36		

3.2.2 Multi-differentiation potential of hAD-MSCs

The multi-differentiation potential of hAD-MSCs such as adipogenic, chondrogenic and osteogenic differentiation were successfully performed. After 14 and 21 days, both control groups grown in the growth medium DMEM and differentiation groups grown in the differentiation medium were fixed, stained, and examined under light microscope. In Figure 3.8, picture A and B stands for chondrogenic differentiation. In Figure 3.8.B, hAD-MSCs were differentiated, and synthesized proteoglycans by chondrocytes which was successfully stained with Alcian Blue while control hAD-MSCs in growth medium was not stained with blue dye in figure 3.8.A after 14 days.

In Figure 3.8, black arrows show the formation of osteocalcin, sign of mineralization in differentiated hAD-MSCs to osteocytes after 21 days. The calcified extracellular matrix in differentiated cells compared to control cells (3.8.C) was stained with Alizarin Red (3.8.D). After 21 days of incubation with adipogenic differentiation medium, hAD-MSCs produced lipid vacuoles stained with Oil Red O was showed with black arrows given in Figure 3.8.F, compared with control group in Figure 3.8.E.

Overall, hAD-MSCs were successfully differentiated into three different cell types; chondrocytes, osteocytes, and adipocytes. In this study, hAD-MSCs had ability to differentiate into different cell types with some stimulator factors which was a characteristic feature of mesenchymal stem cells.

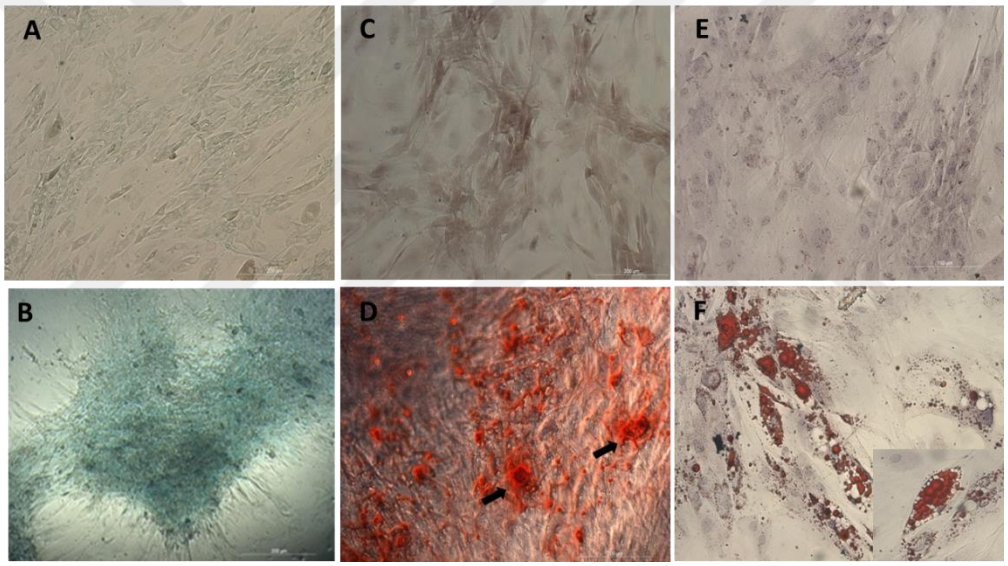

Figure 3.8 : Multi-differentiation potency of hAD-MSCs analyzed by immunohistochemistry (A-B; Chondrogenic potency with Alcian Blue staining after 14 days, C-D; Osteogenic differentiation potency with Alizerin Red Staining after 21 days, E-F; Adipogenic differentiation with Oil Red O staining after 21 days).

3.3 Cardiomyocyte Differentiation of hAD-MSCs by Immunofloresence Assay

The differentiation of hAD-MSCs to cardiomyocyte was characterized by analyzing cardiac markers. After the 10th day of the differentiation process, sarcomeric and ball-like structures on well plate were seen by the microscope.

hAD-MSCs treated with cardiomyocyte differentiation kit were successfully stained with α-actinin, Troponin I, Connexin 43, and Myosin heavy chain

antibodies whereas hAD-MSCs treated with prepared differentiation medium including 5-AZA were slightly stained with the same cardiac markers (Figure 3.9). Even though in the previous cardiomyocyte differentiation studies suggested the use of 5-AZA as a stimulator factor (Carvalho et al., 2012), one of the reason could be the cytotoxic effect of 5-AZA to the cells. Thus, the mortality of adhered cells was seen clearly even after 24 hours of exposure time. Moreover, the control group of hAD-MSCs, only stained with secondary antibody was also not found positive for cardiac markers.

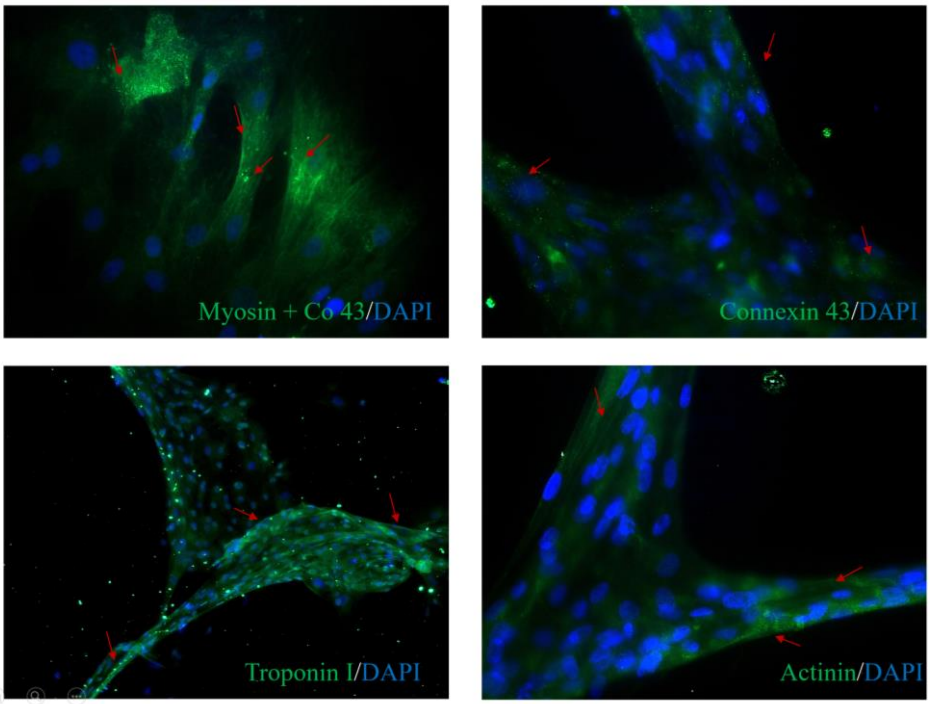

Figure 3.9 : Characterization of cardiac differentiation with cardiac specific markers; α-actinin, Troponin I, Connexin 43, and Myosin heavy chain (all in green). Cell nucleus was stained with DAPI (in blue) by immunofloresence assay after 10 days.

Typical markers for cardiac muscle cells, α-actinin and Connexin 43 were observed in exoskeleton of the cells. Connexin 43 expression was found in both nuclear and cytoplasmic membrane which shows formation of gap junctions. This finding is important and required for the transmission of impulses among cells (Carvalho et al., 2012). The other proteins; myosin heavy chain, α-actinin, and troponin I are important proteins in the contraction of a cardiac muscle and related with the sarcomeric structure of differentiated cells (Lin et al., 2015).

3.4 Cell Proliferation Assay

3.4.1 MTT analysis

The cell viability and proliferation of hAD-MSCs on silk scaffolds were examined by the colorimetric MTT assay. Living cells are metabolically active, and produce reducing compounds such as NADH or NADPH. These compounds reduce the tetrazolium product into a soluble formazan product. From this view, dead cells can't reduce tetrazolium salt. Thus, formation of the formazan product is directly related with the number of viable cells. In the Figure 3.10, dark purple color was observed on the whole surface of silk fibroin scaffolds which reflected the cell viability and proliferation of hAD-MSCs. Since biocompatibility of biomaterial is an important parameter in tissue engineering, this finding could be a promising result for further studies.

The results of MTT assay were used to analyze the effects of silk fibroin scaffolds on hAD-MSCs after 1, 7 and 14 days of incubation shown in Figure 3.11. According to the results, 4 % silk fibroin scaffolds did not have any adverse effect on the cell proliferation, compared with the control cell monolayer without scaffold. It was found to be a biocompatible biomaterial for tissue engineering. The percentage of the cell viability of hAD-MSCs on silk fibroin scaffolds on the day of 1, 7, and 14 days were found to be as 90 %, 118 % and 138 % respectively (Figure 3.11).

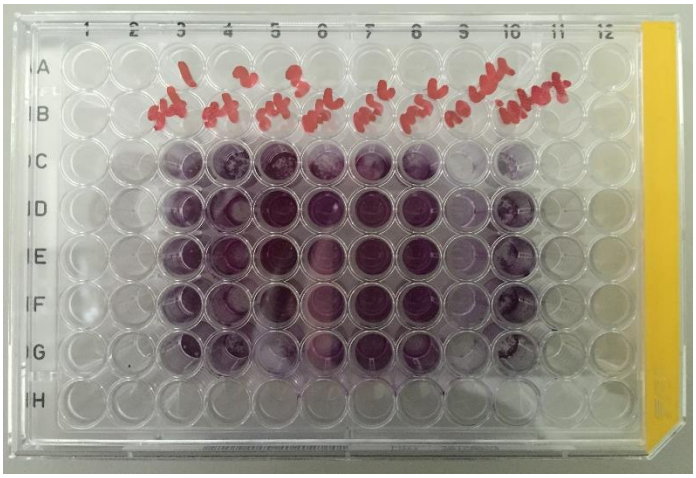

Figure 3.10 : Formation of formazan in dark purple color which represents the number of viable cells.

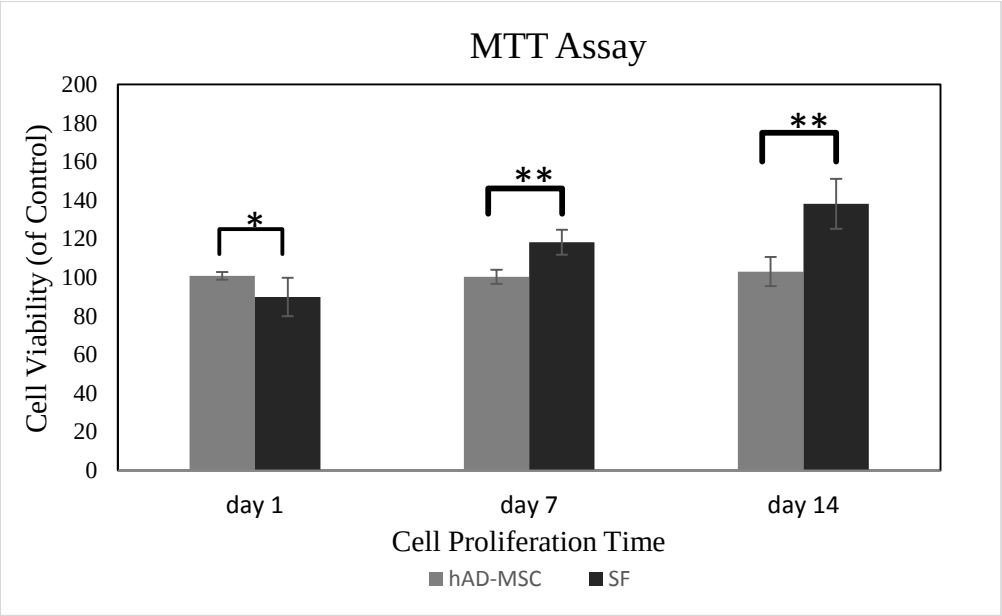

Figure 3.11 : Cellular Metabolic Activity Percentage of 4 % silk scaffolds after 1, 7 and 14 days of incubation (mean±SD, n=3, *p≤0.5, **p≤0.01).

3.4.2 WST-1 cytotoxicity test

The biocompatibility of silk fibroin scaffolds was investigated by the application of direct and indirect contact method. The results of WST-1 assay based on the principle that viable cells have dehydrogenase activity which causes the reduction of the tetrazolium salt WST-1 to formazan. It is a colorimetric assay which changes the color of the medium into dark yellow.

The dark yellow color which directly correlates with the viable cell number was measured at 450 nm. According to the results showed in Figure 3.12., the percentages of cell viability relative to control for the silk fibroin scaffold in both direct and indirect methods were found to be as 92 % and 104 %, relatively. This finding also showed that the silk fibroin scaffold could be thought as a safe biomaterial for further usage in tissue engineering.

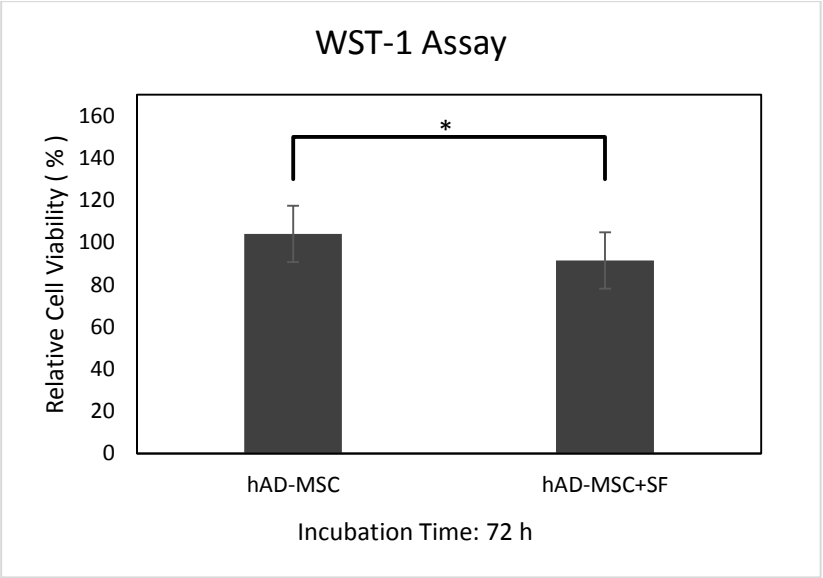

Figure 3.12 : Relative Cell Viability between hAD-MSCs and hAD-MSCs on SF after 72 hours of incubation (mean ± SD, n=1, $p \leq 0.1$).

Live/Dead assay

In Figure 13, the Calcein-AM staining shows the live cells in green while ethidium homodimer-1 (ethD-1) stains dead cells on the fibers of the silk construct. At 1, 7, and 14 days, there were very few dead cells stained with ethD-1 which could not be seen in the merged images (Figure 3.13) in comparison with viable cells.

The live/dead staining of the cells on the scaffolds, positive cell compatibility with the scaffold was seen with Calcein-AM (green) staining. This indicated the spread morphology of the cells. However, the fibers of the silk construct interacted with the ethidium homodimer-1 too. Thus, to determine the reason of red dye is the dead cells or the silk fibers may be a little challenging. In Figure 3.13.g, yellow arrows show dead cells while in figure 3.13.h and 3.13.i arrows show fibers of the silk construct. Since red staining in 3.13.h and 3.13.i shows fibers of the scaffold, live cells spread on porous structure of the scaffold as it was expected.

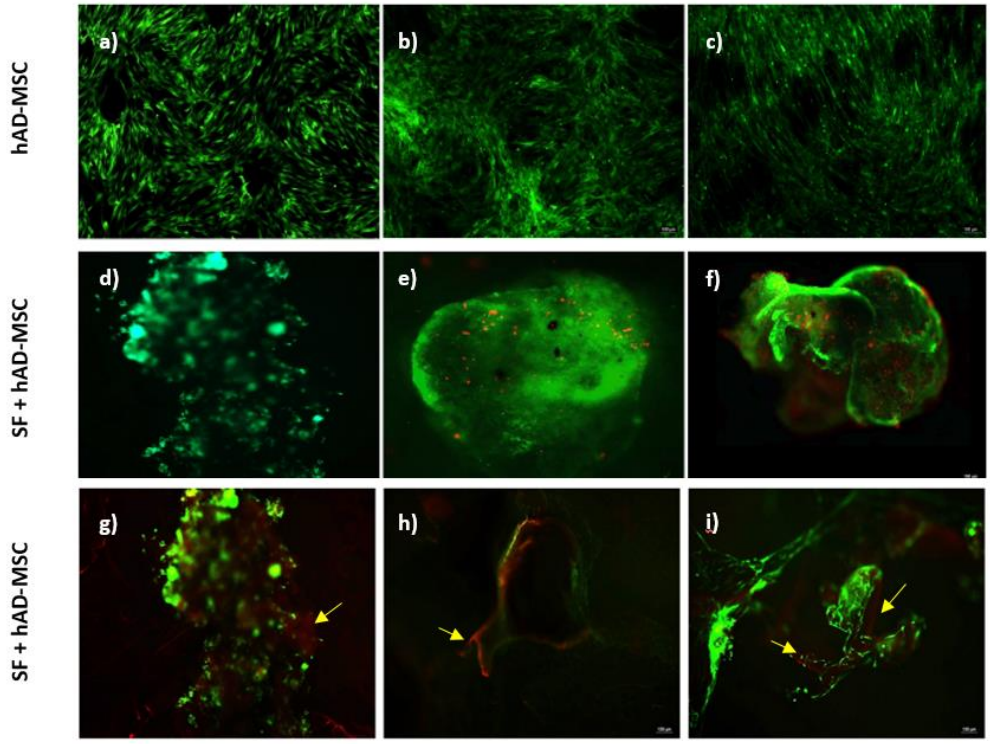

Figure 3.13 : Live/Dead staining of MSCs and hAD-MSCs on silk scaffolds after 1 (a-d-g), 7 (b-e-h), and 14 (c-f-i) days. Viable Cells stained with Calcein AM are shown in green. Dead cells and silk fibers stained with ethidium homodimer-1 are shown in red.

Overall, the morphology of the hAD-MSCs itself and on scaffold was consistent throughout the time points. However, the density of the viable cells was increased as time passed by.

4. CONCLUSION AND RECOMMENDATIONS

The aim of the study was to develop a biodegradable and biocompatible cardiac tissue engineering construct with the help of silk fibroin and adipose derived mesenchymal stem cells. Silk fibroin was chosen as a natural biomaterial because of its good mechanical properties (e.g. high tensile strength), biocompatibility and non-immunogenicity in host. Porosity is an important feature for tissue engineering to sustain tissue growth in 3D scaffolds, so in this study, silk fibroin ratios, 2% and 4%, yielding maximum porosity were selected based on SEM images. Methanol treatment was applied to induce beta sheet structure from rondom coils, and the effect of insulation cover in freezing step before lyophilization was tested. The results showed that insulation cover usage during freezing step, and methanol treatment after lyophilization had a significant role on formation of pore structure so should be optimized carefully.

The water-uptake analysis showed that increasing fibroin concentration decreases water uptake capacity. Thus, 4 % silk fibroin scaffold was chosen to eliminate excessive structural changes during cell culture studies. The biodegradation of silk fibroin scaffold was investigated in the presence of Protease IV enzyme for 14 days. Silk fibroin scaffolds were degraded about 50% ratio until the third day in the enzyme presence whereas only 10% of degradation was observed when no enzyme presents. Biodegradation rate of silk fibroin scaffolds slowed down after the third day. The results suggest that enzymatic activity is an important biodegradation route for silk fibroin.

In the second part of the study, hAD-MSCs were isolated from human adipose tissue, and expanded up to passage number 3. As a result of flow cytometry, more than 90 % of the isolated and expanded cells were characterized as MSC pointing out high level of purity. In the second characterization step, osteogenic, adipogenic and chondrogenic differentiation potential of isolated hAD-MSCs were proven with immunohistochemical

analysis. Mesenchymal stem cell characterization results showed that adipose tissue may be a valuable alternative cell source for tissue engineering approaches.

The biocompatibility of silk fibroin scaffold as a promising medical material was comfirmed by WST-1 assay. In addidition, no adverse effects on cell viability were observed by MTT and Live/Dead assays.

For testing the cardiac differentiation potential of hAD-MSCs, two protocols were followed; i) 5-AZA treatment on hAD-MSCs, and ii) PSC Cardiomyocyte Differentiation Kit. First, 5-AZA as a stimulator factor was tested on hAD-MSCs to differentiate into cardiomyocytes. The result of immunofloresence assay showed that there was no significant staining of cardiac specific markers. Then, PSC Cardiomyocyte Differentiation Kit protocol was followed to sustain cardiac differentiation. After 10 days of incubation, sarcomeric and ball-like structures on well plate were seen under inverted microscope. Immunofloresence assay results proved that differentiated hAD-MSCs were stained with cardiac specific markers such as α-actinin, Troponin I, Connexin 43, and Myosin heavy chain. In conclusion, despite 5-AZA had been an effective treatment for cardiac differentiation in literature, its toxic effect on hAD-MSCs seems to be higher than its differentiation effect on the cells. Moreover, re-differentiation was seen after 10 days of incubation with PSC Cardiomyocyte Differentiation Kit.

Overall, the aim was to fabricate a biodegradable scaffold from natural polymers and to show the potential of this scaffold in cardiac tissue engineering using cardiomyocytes differentiated from hAD-MSCs. Differentiated hAD-MSCs were shown to proliferate on silk fibroin scaffolds with no adverse effect compared with the control cell monolayer without scaffold showing the suitability of this biomaterial for cardiac tissue engineering.

For further analysis, biodegradation rate of silk scaffolds can be extended with the addition of other natural polymers into silk fibroin since it is known that cardiac patches should remain in the body at least two months. Then, morphology of the composite scaffold and pure silk fibroin scaffold can be

compared with SEM analysis in terms of porosity and pore structure. In addition, co-culture with rat cardiomyocytes and mesenchymal stem cells can be performed, and tested on 3D silk fibroin composite material. Finally, a bioreactor can be set up to provide a tissue-specific physiological *in vitro* environment during tissue maturation.

REFERENCES

A. Hokugo, T. Takamoto, and Y. Tabata. (2006). Preparation of hybrid scaffold from fibrin and biodegradable polymer fiber, *Biomaterials 27 61–67*.

Akhyari P., Fedak P.W., Weisel R.D., Lee Y.J., Verma S., Mickle D.A., and Li R-K. (2002). Mechanical stretch regimen enhances the formation of bioengineered autologous cardiac muscle grafts. *Circulation.;106*(12 suppl 1):I-137-I-42.

Askari, A. T., Unzek, S., Popovic, Z. B., Goldman, C. K., Forudi, F., and Kiedrowski, M. (2003). Effect of stromal-cell-derived factor 1 on stem-cell homing and tissue regeneration in ischaemic cardiomyopathy. *Lancet 362, 697– 703.*

Bolooki H.M., and Askari A. (2010). Acute Myocardial Infarction. *Cleveland Clinic: Current Clinical Medicine. 2nd edition. Saunders. Chapter 2*.

Cao, Y., and Wang, B. (2009). Biodegradation of Silk Biomaterials. *International Journal of Molecular Sciences,* 10(4), 1514-1524. doi:10.3390/ijms10041514

Carvalho, Pablo Herthel, Daibert, Ana Paula Falci, Monteiro, Betânia Souza, Okano, Bárbara Silva, Carvalho, Juliana Lott, Cunha, Daise Nunes Queiroz da, Favarato, Lukiya Silva Campos, Pereira, Vanessa Guedes, Augusto, Luis Eugênio Franklin, and Carlo, Ricardo Junqueira Del. (2013). Differentiation of adipose tissue-derived mesenchymal stem cells into cardiomyocytes. *Arquivos Brasileiros de Cardiologia, 100(1),* 82-89.https://dx.doi.org/10.1590/S0066-782X2012005000114

Chen, Q., Harding, S. E., Ali, N. N., Lyon, A. R., and Boccaccini, A. R. (2008). Biomaterials in cardiac tissue engineering: Ten years of research survey. *Materials Science and Engineering: R: Reports*, 59(1-6), 1-37. doi:10.1016/j.mser.2007.08.001

Cheng, K., Kuo, T., Kuo, K., and Hsiao, C. (2011). Human adipose-derived stem cells: Isolation, characterization and current application in regeneration medicine. *Genomic Medicine, Biomarkers, and Health Sciences*, 3(2), 53-62. doi:10.1016/j.gmbhs.2011.08.003

Chomchalao, P., Pongcharoen, S., Sutheerawattananonda, M., and Tiyaboonchai, W. (2013). Fibroin and fibroin blended three-dimensional scaffolds for rat chondrocyte culture. *BioMedical Engineering OnLine*, 12(1), 28. doi:10.1186/1475-925x-12-28

Costa K.D., Lee E.J., and Holmes J.W. (2003). Creating alignment and anisotropy in engineered heart tissue: role of boundary conditions in a model three-dimensional culture system. *Tissue Engineering.* 9(4):567-77.

Dvir, T., Timko, B. P., Kohane, D. S., and Langer, R. (2011). Nanotechnological strategies for engineering complex tissues. *Nature Nanotechnology*, 6, 13-22.

Feng Z, Matsumoto T, and Nakamura T. (2003). Measurements of the mechanical properties of contracted collagen gels populated with rat fibroblasts or cardiomyocytes. J *Artif Organs* 6:192e6.

Jones, G. L., Motta, A., Marshall, M. J., El Haj, A. J., and Cartmell, S. H. (2009). Osteoblast: Osteoclast co-cultures on silk fibroin, chitosan and PLLA films. *Biomaterials*, 30(29), 5376-5384.

Francis, M. P., Sachs, P. C., Elmore, L. W., and Holt, S. E. (2010). Isolating adipose-derived mesenchymal stem cells from lipoaspirate blood and saline fraction. *Organogenesis*, 6(1), 11-14. doi:10.4161/org.6.1.10019

Haifeng Liu, Z.G., Yue Wang, Siew Lok Toh, Vallaya Sutthikkum, and James C.H. Goh, (2006). Modification of sericin-free silk fibers for ligament tissue engineering application. *Journal of Biomedical Materials Research Part B: Applied Biomaterials*, 10: p. 129-138.

H. Fan, H. Liu, E.J.W. Wong, S.L. Toh, and J.C.H. Goh, (2008). In vivo study of anterior cruciate ligament regeneration using mesenchymal stem cells and silk scaffold, *Biomaterials* 29 3324–3337.

J. Perez-Rigueiro, M.E., J. Llorca, and C. Viney, (2001). Tensile Properties of Silkworm Silk Obtained by Forced Silking. *Journal of Applied Polymer Sciences*, 82: p. 1928-1935.

Jin, H., Park, J., Karageorgiou, V., Kim, U., Valluzzi, R., Cebe, P., and Kaplan, D. (2005). Water-stable silk films with reduced β -sheet content. *Advanced Functional Materials*, 15(8), 1241–1247.

Kim, U., Park, J., Kim, H. J., Wada, M., and Kaplan, D. L. (2005). Three-dimensional aqueous-derived biomaterial scaffolds from silk fibroin. *Biomaterials*, 26(15), 2775-2785. doi:10.1016/j.biomaterials.2004.07.044

Kundu, B., Rajkhowa, R., Kundu, S. C., and Wang, X. (2013). Silk fibroin biomaterials for tissue regenerations. *Advanced Drug Delivery Reviews*, 65(4), 457-470. doi:10.1016/j.addr.2012.09.043

Laflamme M.A., and Murry C.E. (2010). Heart regeneration. Nature 2011;473:326e35. Omenetto FG, Kaplan DL. SnapShot: silk biomaterials. *Biomaterials* 2010;31:6119e20.

Lee, M. S., and Makkar, R. R. (2004). Stem-cell transplantation in myocardial infarction: A status report. *Ann Intern Med* 140, 729–737.

Lerdchai, K., Kitsongsermthon, J., Ratanavaraporn, J., Kanokpanont, S., and Damrongsakkul, S. (2016). Thai Silk Fibroin/Gelatin Sponges for the Dual Controlled Release of Curcumin and Docosahexaenoic Acid for

Anticancer Treatment. *Journal of Pharmaceutical Sciences*, 105(1), 221-230. doi:10.1002/jps.24701

Leor, J., Amsalem, Y., and Cohen, S. (2005). Cells, scaffolds, and molecules for myocardial tissue engineering. *Pharmacology & Therapeutics*, 105(2), 151-163. doi:10.1016/j.pharmthera.2004.10.003

Li, M., Ogiso, M., and Minoura, N. (2003). Enzymatic degradation behavior of porous silk fibroin sheets. *Biomaterials*, 24(2), 357-365. doi:10.1016/s0142-9612(02)00326-5

Lin, Z. B., Qian, B., Yang, Y. Z., Zhou, K., Sun, J., Mo, X. M., and Wu, K. H. (2015). Isolation, Characterization and Cardiac Differentiation of Human Thymus Tissue Derived Mesenchymal Stromal Cells. *Journal of Cellular Biochemistry*, 116(7), 1205-1212. doi:10.1002/jcb.25072

Liu, X., and Ma, P. X. (2004). Polymeric Scaffolds for Bone Tissue Engineering. *Annals of Biomedical Engineering*, 32(3), 477-486.

L. Meinel, R. Fajardo, S. Hofmann, R. Langer, J. Chen, B. Snyder, G. Vunjak-Novakovic, and D. Kaplan, (2005). Silk implants for the healing of critical size bone defects, *Bone 37* 688–698.

Lu, S., Wang, X., Lu, Q., Hu, X., Uppal, N., Omenetto, F. G., and Kaplan, D. L. (2009). Stabilization of Enzymes in Silk Films. *Biomacromolecules*, 10(5), 1032-1042. doi:10.1021/bm800956n

Lu, T., Li, Y., and Chen, T. (2013). Techniques for fabrication and construction of three-dimensional scaffolds for tissue engineering. *International Journal of Nanomedicine*, 337. doi:10.2147/ijn.s38635

Lu, Q., Zhang, B., Li, M., Zuo, B., Kaplan, D. L., Huang, Y., and Zhu, H. (2011). Degradation Mechanism and Control of Silk Fibroin. *Biomacromolecules*, 12(4), 1080-1086. doi:10.1021/bm101422j

Brown, J., Lu, C., Coburn, J., and Kaplan, D. L. (2015). Impact of silk biomaterial structure on proteolysis. *Acta Biomaterialia*, 11, 212-221. doi:10.1016/j.actbio.2014.09.013

M. Li, Z. Wu, C. Zhang, S. Lu, H. Yan, D. Huang, and H. Ye. (2001). Study on porous silk fibroin materials. II. Preparation and characteristics of spongy porous silk fibroin materials, *J. Appl. Polym. Sci*. 79 2192–2199.

Mazo M., Gavira J.J., Pelacho B., and Prosper F. (2011). Adipose-derived stem cells for myocardial infarction. *J Cardiovasc Transl Res.* 4(2):145–53.

Meinel L., Hofmann S., Karageorgiou V., Kirker-Head C., McCool J, and Gronowicz G., et al. (2005). The inflammatory responses to silk films in vitro and in vivo. *Biomaterials* 2005;26(2):147–55.

Miniati D.N., and Robbins R.C. (2002). Heart transplantation: A thirty year perspective. *Annu Rev Med* 2002;53:189–205.

Motta, A., Fambri, L. and Migliaresi, C. (2002). Regenerated silk fibroin films: thermal and dynamic mechanical analysis. *Macromol. Chem. Phys. 203*, 1658–1665.

M.R. Alison, R. Poulsom, S. Forbes, N.A. Wright, and J. Pathol. (2002). 197 (4) 419–423.

Ott H.C., Matthiesen T.S., Goh S.K., Black L.D., Kren S.M., and Netoff T.I., et al. (2008). Perfusiondecellularized matrix: using nature's platform to engineer a bioartificial heart. *Nat Med* 2008;14:213e21.

Ozcan, I. (2016). *Construction of A Functional Biodegradable Bone Tissue Engineering Scaffold for Enhanced Biomineralization* (master's thesis). Istanbul Technical University.

Pasumarthi, K. B., and Field, L. J. (2002). Cardiomyocyte cell cycle regulation. *Circ Res 90*, 1044–1054.

Planat-Bénard V., Menard C., and André M., et al. (2004). Spontaneous cardiomyocyte differentiation from adipose tissue stroma cells. *Circ Res.* 2004;94(2):223–9.

Qian, L., and Zhang, H. (2010). Controlled freezing and freeze drying: a versatile route for porous and micro-/nano-structured materials. *Journal of Chemical Technology & Biotechnology*, 86(2), 172-184. doi:10.1002/jctb.2495

A. Vats, N.S. Tolley, J.M. Polak, and L.D.K. Buttery, (2002). *Clin. Otolaryngol.* 27 (4) (2002) 227–232.

Qiang, L. and Zhang, H. (2010). Controlled freezing and freeze drying: a versatile route for porous and micro-/nano-structured materials. *Journal of Chemical Technology and Biotechnology*, 86, 172-184.

Radisic M., Park H., Shing H., Consi T., Schoen F.J., Langer R., Freed L.E., and Vunjak-Novakovic G. (2004). Functional assembly of engineered myocardium by electrical stimulation of cardiac myocytes cultured on scaffolds. *Proceedings of the National Academy of Sciences.* 2004;101(52):18129-34.

Radisic M., Yang L., Boublik J., Cohen R.J., Langer R., and Freed L.E., et al. (2004). Medium perfusion enables engineering of compact and contractile cardiac tissue. *Am J Physiol Heart Circ Physiol* 2004;286:H507e16.

Rinaldi, A. M. (2014). *Optimization of silk scaffold for cardiac tissue engineering* (master's thesis). Tufts University. Retrieved from http://gradworks.umi.com/15/67/1567108.html

Severs, N.J. (2000). The cardiac muscle cell. *Bioessays* 22, 188

Silk Fibroin-Lessons -Tes Teach. (n.d.). (2017). https://www.tes.com/lessons/xgx8VfOSYlkF4w/silk-fibroin

Smits, P. C., van Geuns, R. J., Poldermans, D., Bountioukos, M., Onderwater, E. E., and Lee, C. H., et al. (2003). Catheter-Based intramyocardial injection of autologous skeletal myoblasts as a primary treatment of ischemic heart failure. Clinical experience with six-month follow-up. *J Am Coll Cardiol 42*, 2063– 2069.

Sun, Y., Kiani, M. F., Postlethwaite, A. E., and Weber, K. T. (2002). Infarct scar as living tissue. *Basic Res Cardiol* 97, 343– 347.

Talukdar S., Mandal M., Hutmacher D.W., Russell P.J., Soekmadji C., and Kundu S.C. (2011). Engineered silk fibroin protein 3D matrices for in vitro tumor model. *Biomaterials* 2011;32:2149e59.

Talukdar S., Nguyen Q.T., Chen A.C., Sah R.L., and Kundu S.C. (2011). Effect of initial cell seeding density on 3D-engineered silk fibroin scaffolds for articular cartilage tissue engineering. *Biomaterials* 2011;32:8927e37.

Thomson, J. A., Itskovitz-Eldor, J., Shapiro, S. S., Waknitz, M. A., Swiergiel, J. J., and Marshall, V. S., et al. (1998). Embryonic stem cell lines derived from human blastocysts. *Science 282*, 1145– 1147.

Vacanti, J. P., and Langer, R. (1999). Tissue engineering: The design and fabrication of living replacement devices for surgical reconstruction and transplantation. *Lancet 354*(Suppl. 1), SI32– S34.

Vulliet, P. R., Greeley, M., Halloran, S. M., MacDonald, K. A., and Kittleson, M. D. (2004). Intra-coronary arterial injection of mesenchymal stromal cells and microinfarction in dogs. *Lancet 363*, 783– 784.

Vunjak-Novakovic, G., Tandon, N., Godier, A., Maidhof, R., Marsano, A., Martens, T. P., and Radisic, M. (2010). *C*hallenges in Cardiac Tissue Engineering. *Tissue Engineering Part B: Reviews*,16(2), 169-187. doi:10.1089/ten.teb.2009.0352

Wang Y., Singh A., Xu P., Pindrus M.A., Blasioli D.J., and Kaplan D.L. (2006). Expansion and osteogenic differentiation of bone marrow-derived mesenchymal stem cells on a vitamin C functionalized polymer. *Biomaterials* 2006;27:3265e73.

Wang, Y.Z., Rudym, D.D., Walsh, A., Abrahamsen, L., Kim, H.J., Kim, H.S., Kirker-Head, C., and Kaplan, D.L. (2008). In vivo degradation of three-dimensional silk fibroin scaffolds. *Biomaterials* 2008,29, 3415-3428

Rockwood, D. N., Preda, R. C., Yücel, T., Wang, X., Lovett, M. L., and Kaplan, D. L. (2011). Materials fabrication from Bombyx mori silk fibroin. *Nature Protocols*, 6(10), 1612-1631. doi:10.1038/nprot.2011.379

Willerth S.M., Sakiyama-Elbert S.E. (2008). Combining stem cells and biomaterial scaffolds for constructing tissues and cell delivery. In: Girard Lisa, editor. Stembook; 2008. doi/10.3824/stembook.1.1.1.

Wongnarat, C., and Srihanam, P. (2013). Degradation Behaviors of Thai Bombyx mori Silk Fibroins Exposure to Protease Enzymes. *Engineering, 05(01)*, 61-66. doi:10.4236/eng.2013.51010

Yan, L., Oliveira, J. M., Oliveira, A. L., Caridade, S. G., Mano, J. F., and Reis, R. L. (2012). Macro/microporous silk fibroin scaffolds with potential for articular cartilage and meniscus tissue engineering applications. *Acta Biomaterialia*, 8(1), 289-301. doi:10.1016/j.actbio.2011.09.037

Yoon, Y. S., Park, J. S., Tkebuchava, T., Luedeman, C., and Losordo, D. W. (2004). Unexpected severe calcification after transplantation of bone marrow cells in acute myocardial infarction. *Circulation* (01.CIR.0000134696.0000108436.0000134665).

Zimmermann W.H., Melnychenko I., Wasmeier G., Didie M., Naito H., and Nixdorff U., et al. (2006). Engineered heart tissue grafts improve systolic and diastolic function in infarcted rat hearts. *Nat Med* 2006;12:452e8.

Zuk, P. A., Zhu, M., Mizuno, H., Huang, J., Futrell, J. W., Katz, A. J., Benhaim, P., Lorenz, H. P. and Hedrick, M. H. (2001). Multilineage cells from human adipose tissue: implications for cell-based therapies. *Tissue Eng.* 7, 211-228.

Zuk, P. A., Zhu, M., Ashjian, P., De Ugarte, D. A., Huang, J. I., Mizuno, H., Alfonso, Z. C., Fraser, J. K., Benhaim, P. and Hedrick, M. H., (2002). Human Adipose Tissue Is a Source of Multipotent Stem Cells. *Mol Biol Cell. 1*3, 4279-4295.99

APPENDICES

APPENDIX A: Chemicals and Materials

APPENDIX B: Laboratory Equipment

APPENDIX C: Preparation of 1X Phosphate Buffered Saline (PBS) Buffer

APPENDIX A

Chemical/Material (ITU)	Supplier
Methanol, CH_3OH	Sigma-Aldrich
Sodium azide, NaN_3	Merck Millipore
Silkworm cocoons	Kozabirlik
Sodium chloride, NaCl	Merck Millipore
Potassium chloride, KCl	Sigma-Aldrich
Sodium phosphate dibasic, Na_2HPO_4	Sigma-Aldrich
Potassium phosphate monobasic, KH_2PO_4	Sigma-Aldrich
Lithium bromide, LiBr	Sigma-Aldrich
Sodium sulphate, Na_2SO_4	Sigma-Aldrich
Sodium bicarbonate, $CHNaO_3$	Sigma-Aldrich
Calcium chloride, $CaCl_2$	Sigma-Aldrich
Sodium carbonate, Na_2CO_3	Sigma-Aldrich
Hydrochloride, HCl	Sigma-Aldrich
Sodium hydroxide, NaOH	Sigma-Aldrich
Protease XIV	Sigma-Aldrich

APPENDIX A-cont

Chemical/Material (TUBITAK)	**Supplier**
2-mercaptoethanol	Bio-Rad
5-azacytidine	Biochem
Alcian Blue	Sigma-Aldrich
Alizarin Red S Staining Kit	Sciencell
ACF Chondrogenic Differentiation Medium	MesenCult™
Adipogenic Differentiation Medium (Human)	MesenCult™
Anti-Cardiac Troponin I antibody	ABCAM
Anti-heavy chain cardiac Myosin antibody	ABCAM
Anti-Rabbit IgG Alexa Flour 488 conjugate	Cell Signaling
Antibiotic-Antimycotic (100X)	GIBCO
APC anti-human CD73 (Ecto-5'-nucleotidase) Antibody	Biolegend
Cardiomyocyte Differentiation Kit	Thermo Fisher Scientific
Chondrogenic Differentiation Kit	MesenCult™
Collagenase, Type I, powder	Gibco
Collagenase, Type II, powder	Gibco
Corning® Costar® Ultra-Low attachment multiwell plate	Sigma-Aldrich
Dexamethasone	Sigma-Aldrich
Dimethyl Sulfoxide (DMSO)	Santa Cruz
DMEM-lg	GIBCO
DPBS	GIBCO-Invitrogen
Insulin-Transferrin-Selenium (ITS -G)	GIBCO
Fetal Bovine Serum	GIBCO
FITC anti-human CD90 (Thy1) Antibody Clone 5E10	Biolegend
Formalin solution, neutral buffered, 10%	Sigma-Aldrich
GlutaMAX™ Supplement	GIBCO
Goat Anti-Mouse IgG H&L (Alexa Fluor® 488)	ABCAM
Human anti-sarcomeric-α-actin antibody	ABCAM
L-Ascorbic acid	Sigma-Aldrich
Live/Dead Cytotoxicity Kit	Thermo Fisher Scientific
L-Glutamine	Gibco
MEM NEAA	Gibco
NH_4Cl	Sigma-Aldrich
Oil Red O Staining Kit	Lifeline
Osteogenic Stimulatory Kit (Human)	MesenCult™
PerCP/Cy5.5 anti-human CD105 Antibody	Biolegend
PE anti-human CD45 Antibody	Biolegend
PE anti-human CD34 Antibody	Biolegend
PE anti-human CD11b Antibody	Biolegend
Rabbit -α-actin antibody	Cell Signaling
Rabbit Ab Anti-Connexin 43 antibody	Cell Signaling
Recombinant Human TGF-beta 1 R&D systems	R&D Systems
Safranin O	Sigma-Aldrich
Trypsin-EDTA Solution 1X 0.25%	Gibco
Von Kossa Stain Kit	American Master Tech
WST-1	Roche

APPENDIX B

Equipment	Supplier
Refrigerator, +4 ^{o}C	Vestel
Freezer, - 86 ^{o}C	Thermo Scientific
Magnetic stirrer	Cole-Parmer
Inverted Phase Contrast Microscope	Nikon TMS
Fully Automated Inverted Research Microscope	Leica CTR 6000
Incubator	Esco Cell Culture
Scale	Precisa Gravimetrics AG
Orbital Shaker	Thermo Scientific
Freezer, -20 ^{o}C	Arçelik
Freeze-dryer	Martin Christ
pH metre	WTW GmbH
Rocking platform shaker	Heidolph Instruments
Heating/Drying oven	Memmert GmbH + Co. KG
Biological Safety Cabinet	Esco Sentinel™
Centrifuge	Beckman Coulter
Centrifuge	Hettich Universal
Cover Glasses, Circles	Superior
Mini centrifuge	*GmCLab, Gilson*
Microplate Reader	BioTek
Pipettes	Eppendorf
Beakers	ISOLAB
Tissue culture flask 75, 150 cm²	TPP Techno Plastic Products AG
Tissue culture test plate, 24 & 96 wells	TPP Techno Plastic Products AG
Serological pipettes sterile 2,5,10,25ml	Greiner
Scanning electron microscope, SEM	FEI
Dialysis cassettes	Thermo Scientific
Syringe and needle	BD Medical
Ultrapure water system	TKA-Pacific
Water bath	Techne

APPENDIX C

To prepare 1 L 1 M p.H 7.4 PBS;

- 8 g of sodium chloride (NaCl)
- 0.2 g of potassium chloride (KCl)
- 1.44 g of sodium phosphate dibasic (Na2HPO4)
- 0.24 g of potassium phosphate monobasic (KH2PO4)

were weighed and dissolved in 800 mL ultrapure water. The pH of the solution was adjusted to 7.4 with hydrochloride (HCl). Then, total volume of the solution was adjusted to 1 liter with ultrapure water. In the end, the solution was sterilized by filtration.

CURRICULUM VITAE

Name Surname : Gizem Merve ŞAHİN

Place and Date of Birth : Ankara, 5 September 1989

E-Mail : g.mervesahin@hotmail.com

EDUCATION :

- **B.Sc.** : 2012, Istanbul Technical University & Montana State University, Chemical and Metallurgical Engineering Faculty, Department of Bioengineering

PROFESSIONAL EXPERIENCE AND REWARDS:

- Researcher, TUBITAK-TUSSIDE Health Economics & Healthcare Management R&D (May 2013 - March 2016)
- R&D Project Responsible, Occlutech Tıbbi Ürünler (April 2017 - Present)
- BIOMED 2017, Poster presentation: M.G.SAHİN, F.N.KÖK, Y. CETİN "Cardiomyocyte Differentiation of Human Adipose-Derived Mesenchymal Stem Cells on Silk Fibroin Scaffolds" Mayıs 2017, Ankara-TURKEY